

Individual Migration Pathways of Modern Planktic Foraminifers: Chamber-by-Chamber Assessment of Stable Isotopes

Authors: Takagi, Haruka, Moriya, Kazuyoshi, Ishimura, Toyoho, Suzuki, Atsushi, Kawahata, Hodaka, et al.

Source: Paleontological Research, 20(3) : 268-284

Published By: The Palaeontological Society of Japan

URL: <https://doi.org/10.2517/2015PR036>

The BioOne Digital Library (<https://bioone.org/>) provides worldwide distribution for more than 580 journals and eBooks from BioOne's community of over 150 nonprofit societies, research institutions, and university presses in the biological, ecological, and environmental sciences. The BioOne Digital Library encompasses the flagship aggregation BioOne Complete (<https://bioone.org/subscribe>), the BioOne Complete Archive (<https://bioone.org/archive>), and the BioOne eBooks program offerings ESA eBook Collection (<https://bioone.org/esa-ebooks>) and CSIRO Publishing BioSelect Collection (<https://bioone.org/csiro-ebooks>).

Your use of this PDF, the BioOne Digital Library, and all posted and associated content indicates your acceptance of BioOne's Terms of Use, available at www.bioone.org/terms-of-use.

Usage of BioOne Digital Library content is strictly limited to personal, educational, and non-commercial use. Commercial inquiries or rights and permissions requests should be directed to the individual publisher as copyright holder.

BioOne is an innovative nonprofit that sees sustainable scholarly publishing as an inherently collaborative enterprise connecting authors, nonprofit publishers, academic institutions, research libraries, and research funders in the common goal of maximizing access to critical research.

Individual migration pathways of modern planktic foraminifers: Chamber-by-chamber assessment of stable isotopes

HARUKA TAKAGI¹, KAZUYOSHI MORIYA², TOYOHO ISHIMURA^{3*}, ATSUSHI SUZUKI³,
HODAKA KAWAHATA⁴ AND HIROMICHI HIRANO²

¹Graduate School of Creative Science and Engineering, Waseda University, 1-6-1 Nishiwaseda, Shinjuku, Tokyo 169-8050, Japan
(e-mail: harurah-t@fuji.waseda.jp)

²Department of Earth Sciences, School of Education, Waseda University, 1-6-1 Nishiwaseda, Shinjuku, Tokyo 169-8050, Japan

³Geological Survey of Japan, National Institute of Advanced Industrial Science and Technology, 1-1-1 Higashi, Tsukuba, Ibaraki 305-8567, Japan
Atmosphere and Ocean Research Institute, The University of Tokyo, 5-1-5 Kashiwanoha, Kashiwa, Chiba 277-8564, Japan

*Present address: Department of Chemistry and Material Engineering, National Institute of Technology, Ibaraki College, 866 Nakane, Hitachinaka, Ibaraki 312-8508, Japan

Received August 17, 2015; Revised manuscript accepted November 23, 2015

Abstract. The stable carbon ($\delta^{13}\text{C}$) and oxygen isotopes ($\delta^{18}\text{O}$) of planktic foraminiferal tests have been widely used as proxies in paleoceanography and paleoclimatology. The ontogenetic isotopic profiles of foraminifers are also thought to record ecological information about species, such as changes in habitat depth and symbiotic relationships. However, isotopic profiles during “individual ontogeny” have rarely been examined. In this study, we report the ontogenetic isotopic information for three net-collected modern species, *Globigerinoides sacculifer*, *Neogloboquadrina dutertrei*, and *Globorotalia inflata*, together with several *in situ* oceanographic parameters of the water column in Sagami Bay, Japan (seawater temperature, salinity, nutrients, chlorophyll *a* content, $\delta^{13}\text{C}$ of dissolved inorganic carbon [DIC], and $\delta^{18}\text{O}$ of seawater). We examined the ontogenetic profiles of the foraminifers with chamber dissection and chamber-by-chamber analyses of $\delta^{13}\text{C}$ and $\delta^{18}\text{O}$ using a specially designed continuous-flow mass spectrometry system. The ontogenetic $\delta^{18}\text{O}$ profiles showed overall ^{18}O -enrichment in all three species, suggesting their ontogenetic migration toward deeper habitats. When these records were compared with the physicochemical profiles of the water column, all the ontogenetic records began within the uppermost thermocline or shallower, corresponding to the depth of relatively high chlorophyll content. Later in ontogeny, *Gs. sacculifer* and *N. dutertrei* migrated to the bottom of the level of maximum chlorophyll, whereas *Gr. inflata* descended to a depth of 200 m. The deviations of foraminiferal $\delta^{13}\text{C}$ from the $\delta^{13}\text{C}$ of DIC were largest in the juvenile stages, but were near zero at a test mass of *ca.* 10 μg for all three species. Contrary to the subsequent asymptotic profiles of this deviation in *N. dutertrei* and *Gr. inflata*, *Gs. sacculifer* alone showed a subsequent increase, of up to +1.0‰, reflecting its symbiotic relationship. We conclude that a certain ontogenetic test mass, in this case of around 10 μg , can be assigned to a preferable size class of foraminifers from which to reconstruct the paleo- $\delta^{13}\text{C}$ of DIC in the water column, regardless of the species ecology.

Key words: habitat depth, ontogenetic migration, planktic foraminifers, stable carbon isotope, stable oxygen isotope

Introduction

The analysis of geochemical traits using foraminiferal tests has enhanced our understanding in the fields of paleoceanography, paleoclimatology, and paleoecology (e.g. Emiliani, 1955; Berger *et al.*, 1978; Norris, 1996; Zachos *et al.*, 2001). Since Emiliani (1954) first analyzed stable carbon ($\delta^{13}\text{C}$) and oxygen isotopes ($\delta^{18}\text{O}$) in the

calcite tests of foraminifers, they have been used widely and are now one of the best developed tools for evaluating environments in deep time. Their use is grounded in the well established idea that the isotopic composition of biogenic calcium carbonate, including foraminiferal calcite, reflects the physicochemical conditions under which it formed (Urey, 1947; Emiliani, 1954, 1955; Bemis *et al.*, 1998). It is noteworthy that paleoceanographic anal-

yses using planktic foraminiferal tests are based on a knowledge of the ecology of modern foraminifers, especially the segregation of their habitat by depth in the vertical structure of the water column. For example, the thermal stratification in the Holocene was reconstructed using the oxygen isotopic composition of multiple species of planktic foraminifers living at different depths (e.g. Mulitza *et al.*, 1997; Mortyn *et al.*, 2002). These data have also been used in studies of paleoproductivity, in which carbon isotopic gradients are established between species that live in the mixed surface layer and those that live below the thermocline (Mulitza *et al.*, 1998). These studies would not be possible without a knowledge of the habitat depths of the species analyzed. The species habitat depth has been verified with field observations using depth-discrete plankton tows (e.g. Fairbanks *et al.*, 1980, 1982; Kuroyanagi and Kawahata, 2004).

In addition to the vertical habitat segregation of adult specimens, a number of studies using depth-discrete plankton tows have reported that planktic foraminifers migrate vertically to some extent throughout their ontogeny (e.g. Erez *et al.*, 1991; Bijma and Hemleben, 1994). Because the tests of planktic foraminifers are composed of about a dozen chambers, secreted one by one, the test potentially contains within this series of chambers a set of environmental information about the water column. Theoretically, we can decode that information from a single foraminiferal test if we analyze the geochemical proxies recorded in each chamber individually. Conversely, when the environmental conditions of a water column are known, we can reconstruct the migration pathways of foraminifers throughout their ontogeny. Such ontogenetic data sets for specific species have conventionally been obtained by analyzing a series of size-fractionated tests for each species (Ravelo and Fairbanks, 1992, 1995; Norris, 1996; Wilke *et al.*, 2006; Friedrich *et al.*, 2012; Birch *et al.*, 2012, 2013). However, for a small size fraction (e.g. <150 μm) it is often difficult to identify the smaller specimens to the species level, and to collect enough individuals (amount of carbonate) for the isotopic analysis. These challenges may make it difficult to obtain the hypothetical ontogenetic series of geochemical profiles. On the contrary, a series of chambers within an individual test undoubtedly shows the actual ontogenetic order. Besides the stable isotopic studies, single chamber Mg/Ca measurements using laser ablation inductively coupled plasma mass spectrometry (LA-ICP-MS) technique has increasingly been being used as a tool to reconstruct depth migration of planktic foraminifers recently (e.g. Eggins *et al.*, 2003; Steinhardt *et al.*, 2014, 2015a).

In this study, we present the chamber-by-chamber

$\delta^{13}\text{C}$ and $\delta^{18}\text{O}$ records of modern planktic foraminifers, together with *in situ* environmental parameters on the water column, including the temperature, salinity, nutrients, chlorophyll *a* content, carbon isotopes of dissolved inorganic carbon ($\delta^{13}\text{C}_{\text{DIC}}$), and oxygen isotopes of seawater ($\delta^{18}\text{O}_{\text{sw}}$). The aim was to determine where in the water column the foraminifers calcified each chamber throughout their ontogeny by estimating the calcifying temperatures from the $\delta^{18}\text{O}$ records. We also discuss the deviation of the test $\delta^{13}\text{C}$ from that of dissolved inorganic carbon (DIC) at the calculated calcification depth to identify preferable species and/or ontogenetic stages that reflect $\delta^{13}\text{C}_{\text{DIC}}$. We also evaluated the possible causes of these deviations from equilibrium $\delta^{13}\text{C}$.

Materials and methods

Foraminifers and water sampling

Samples were collected in Sagami Bay, Kanagawa, Japan (35°05'N, 139°28'E; water depth, 920 m) on 11 October 2011 (Figure 1). The planktic foraminifers were collected with a closing plankton net (aperture opening, 30 cm; 100 μm mesh; Marukawa Closing Plankton Net, Rigosha, Tokyo, Japan). The net was towed vertically through the water over specific intervals between 0 and 600 m (i.e., 0–20, 0–33, 0–40, 0–50, 0–100, 0–200, 40–400, 0–400, and 0–600 m). Seawater samples were collected at depths of 0, 10, 20, 33, 40, 50, 100, 200, 400, and 600 m. Seawater samples for analyses of $\delta^{13}\text{C}_{\text{DIC}}$ and $\delta^{18}\text{O}_{\text{sw}}$ were collected in 100 mL glass vials and sealed onboard without bubbles. To prevent the biological consumption of carbon, mercuric chloride was added to the vials of water for $\delta^{13}\text{C}_{\text{DIC}}$ analysis before they were sealed. Other water samples for nutrient analysis were filtered with a cellulose acetate filter (pore size of 0.45 μm) immediately after collection. These aliquots were kept frozen until analysis (see below for details). The vertical distributions of temperature, salinity, and chlorophyll fluorescence were measured with a conductivity–temperature–depth sensor (Compact-CTD, JFE Advantech, Hyogo, Japan) in the water column at depths of <600 m.

Foraminiferal analyses

The net-collected samples were washed with tap water and then soaked in 12% sodium hypochlorite solution overnight to decompose the organic matter. The samples were then rinsed through a 63 μm sieve with tap water. Three species of planktic foraminifers with different ecologies were analyzed: *Globigerinoides sacculifer* ($n = 5$), *Neogloboquadrina dutertrei* ($n = 4$), and *Globorotalia inflata* ($n = 3$). *Globigerinoides sacculifer* was selected as representative of shallow-dwelling species with sym-

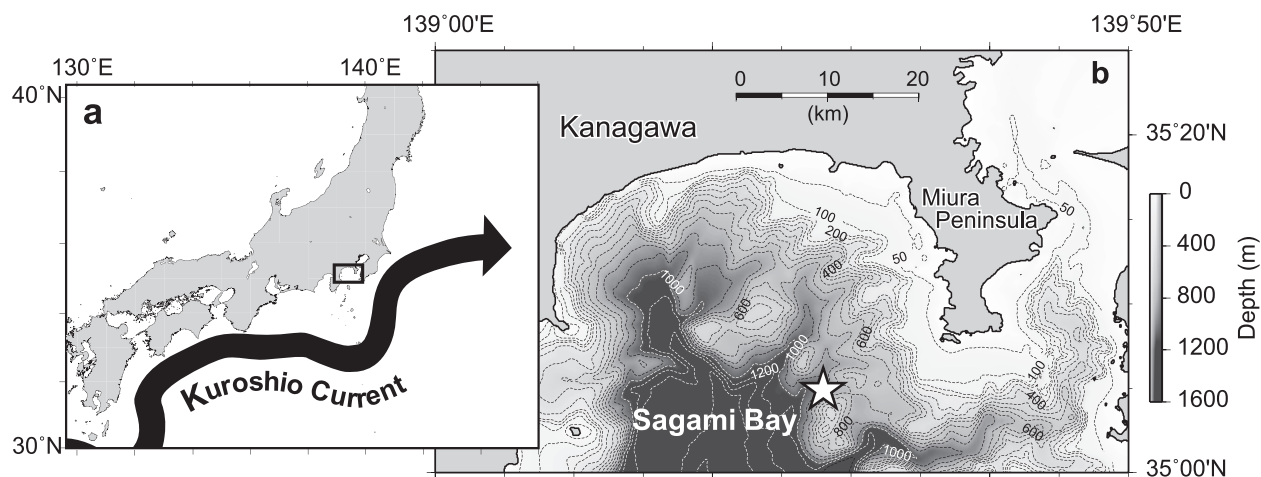


Figure 1. a, Map showing the position of the Kuroshio Current on the sampling day (11 October 2011), and the study area (rectangle), which is enlarged in panel b. b, Map showing the bathymetry of Sagami Bay. The open star shows the location of the sampling site (35°05'N, 139°28'E; water depth, 920 m).

biotic algae (e.g. Bé, 1977; Erez and Honjo, 1981; Birch *et al.*, 2013). This is one of the best-studied species of planktic foraminifers, especially in terms of its ecology and the isotope characteristics of its test (e.g. Bé *et al.*, 1981; Caron *et al.*, 1981; Spero and Lea, 1993). *Neogloboquadrina dutertrei* was selected as a general intermediate-dwelling species (e.g. Bé, 1977; Erez and Honjo, 1981). *Globorotalia inflata* was selected as representative of deep-dwelling *Globorotalia* species without symbionts (e.g. Bé, 1977; Erez and Honjo, 1981). The specimens of these species were picked under a stereoscopic microscope and selected specimens were dissected into chambers with ophthalmic surgical microblades (Feather Safeshield Incision Scalpel 15° Angle, Feather, Osaka, Japan) (Figure 2). The dissection of the chambers was continued until the remaining test became too small to dissect (Figure 2d; see Takagi *et al.*, 2015 for details). The $\delta^{13}\text{C}$ and $\delta^{18}\text{O}$ values for each chamber were analyzed with a customized continuous-flow isotope ratio mass spectrometry system at the Geological Survey of Japan, Advanced Industrial Science and Technology (AIST) (for details of the system, see Ishimura *et al.*, 2004, 2008). Each dissected chamber was reacted with anhydrous phosphoric acid at 25°C. To calculate the CaCO_3 mass of the sample, the pressure of the manually purified CO_2 gas in the fixed volume of the vacuum line was measured. The CO_2 gas was then introduced to the isotopic ratio mass spectrometer (Isoprime, Isoprime Ltd., Stockport, UK) with helium carrier gas. The system determines both $\delta^{13}\text{C}$ and $\delta^{18}\text{O}$ values for microvolumes of carbonate samples as small as 1.0 μg , with external precision better than $\pm 0.1\text{‰}$. The NBS-19

carbonate standard was used for calibration of the Vienna Pee Dee belemnite (VPDB) scale.

Analyses of water samples

To determine $\delta^{13}\text{C}_{\text{DIC}}$ and $\delta^{18}\text{O}_{\text{sw}}$, the CO_2 gas generated from and equilibrated with each seawater sample was analyzed. An aliquot (20 mL) of each seawater sample was injected into an evacuated glass vial containing amidosulfonic acid. All the DIC in the seawater was converted to CO_2 . The vials were shaken in a water bath at 25°C overnight to equilibrate the $\delta^{18}\text{O}$ of the seawater with that of the CO_2 gas generated. The dual inlet system of the mass spectrometer (Isoprime) at AIST was used for the analysis, which determines the $\delta^{13}\text{C}$ and $\delta^{18}\text{O}$ with analytical error of $\pm 0.1\text{‰}$. The $\delta^{18}\text{O}_{\text{sw}}$ values were reported relative to Vienna Standard Mean Ocean Water (VSMOW).

The concentrations of nitrate (NO_3), nitrite (NO_2), phosphate (PO_4), and silicate (SiO_4) were determined with a colorimetric analysis in a continuous flow system at Ehime University (AutoAnalyzer 3, Bran + Luebbe, Norderstedt, Germany). The water samples for chlorophyll *a* analysis (1 L) were filtered through Whatman GF/F glass fiber filters within 5 h of collection, and the filters were then immediately soaked in 10 mL of *N,N*-dimethylformamide (DMF) in dark glass vials for more than 24 h. The chlorophyll *a* concentration in the DMF extract was measured with a fluorometer at Ehime University (10AU, Turner Design, California, USA).

Estimation of calcification depth

Based on the $\delta^{18}\text{O}_{\text{sw}}$ values determined and the tem-

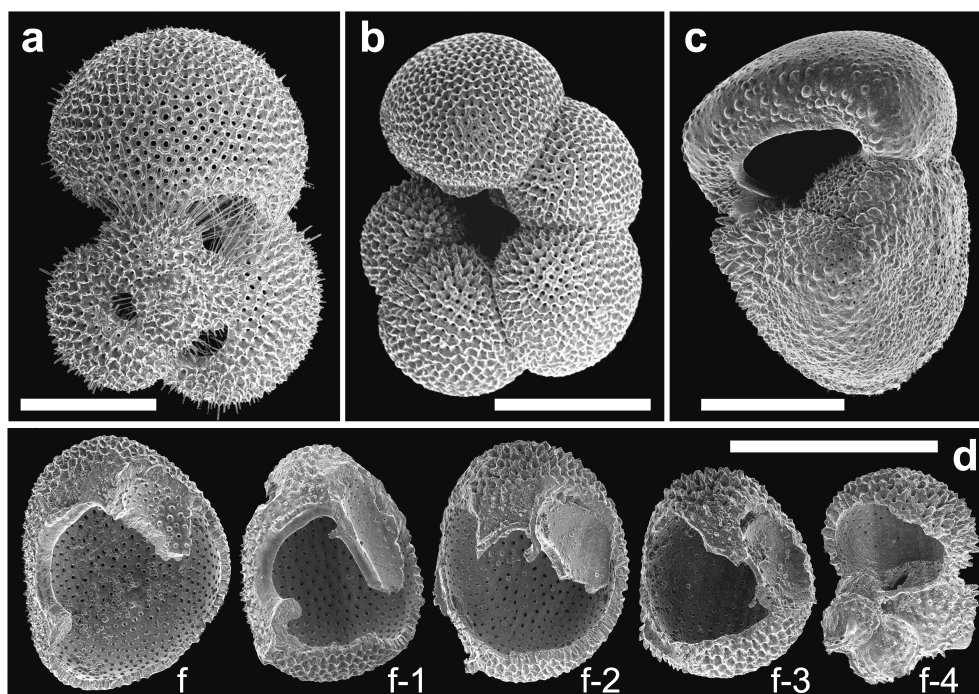


Figure 2. Scanning electron micrographs of the species used in this study, and an example of a series of dissected chambers. **a**, *Globigerinoides sacculifer*; **b**, *Neogloboquadrina dutertrei*; **c**, *Globorotalia inflata*; **d**, Dissected chambers of *Neogloboquadrina dutertrei* (specimen dut2). f, f-1, f-2, ... indicate the chamber positions counting backward from the final chamber (f). Scale bars are 200 μm .

peratures measured in the water column, we calculated the expected oxygen isotope values for the inorganic calcite precipitated in equilibrium with seawater ($\delta^{18}\text{O}_{\text{eq}}$). We used the equation of Kim and O'Neil (1997), which was established for inorganic calcite precipitated in a temperature range of 10–40°C:

$$1000 \ln \alpha = 18.03 \times (10^3 T_k^{-1}) - 32.42 \quad (1)$$

where α is the fractionation factor between CaCO_3 (inorganic calcite) and H_2O (seawater), and T_k is the seawater temperature in degrees Kelvin (K). The fractionation factor can be written using delta notation:

$$\alpha = (\delta^{18}\text{O}_{\text{eq}} + 1000) / (\delta^{18}\text{O}_{\text{sw}} + 1000) \quad (2)$$

where $\delta^{18}\text{O}_{\text{eq}}$ and $\delta^{18}\text{O}_{\text{sw}}$ are relative to the VSMOW standard. The values of $\delta^{18}\text{O}_{\text{eq}}$ (VSMOW) were converted to the VPDB scale as follows (Coplen *et al.*, 1983):

$$\delta^{18}\text{O}_{\text{eq}} (\text{VPDB}) = (0.970017 \times \delta^{18}\text{O}_{\text{eq}} (\text{VSMOW})) - 29.98 \quad (3)$$

We estimated the $\delta^{18}\text{O}_{\text{eq}}$ -derived calcification depth for each chamber analyzed, assuming that the foraminiferal

chambers were precipitated under isotopic equilibrium with seawater.

Many authors have proposed species-specific relationships among calcification temperature and $\delta^{18}\text{O}_{\text{sw}}$, and the $\delta^{18}\text{O}$ value of the foraminiferal test, indicating that there is a small vital effect on the $\delta^{18}\text{O}$ of foraminiferal calcite (Erez and Luz, 1983; Bouvier-Soumagnac and Duplessy, 1985; Bemis *et al.*, 1998; Mulitza *et al.*, 2003; Spero *et al.*, 2003). For comparison, we also calculated the species-specific $\delta^{18}\text{O}$ of the foraminifers using equations that were most recently established:

$$\delta^{18}\text{O}_{G_{SS}} = (12.0 - T) / 5.67 + (\delta^{18}\text{O}_{\text{sw}} - 0.27) \quad (4)$$

(Spero *et al.*, 2003)

$$\delta^{18}\text{O}_{Nd} = (10.5 - T) / 3.58 + (\delta^{18}\text{O}_{\text{sw}} - 0.20) \quad (5)$$

(Bouvier-Soumagnac and Duplessy, 1985)

$$\delta^{18}\text{O}_{Grm} = (14.9 - T) / 5.13 + (\delta^{18}\text{O}_{\text{sw}} - 0.27) \quad (6)$$

(Spero *et al.*, 2003)

where $\delta^{18}\text{O}_{G_{SS}}$, $\delta^{18}\text{O}_{Nd}$, and $\delta^{18}\text{O}_{Grm}$ represent the expected species-specific $\delta^{18}\text{O}$, T is the seawater temperature in degrees Celsius ($^{\circ}\text{C}$), and -0.27 in eqs. (4) and (6) and -0.20 in eq. (5) are the conversion-correction val-

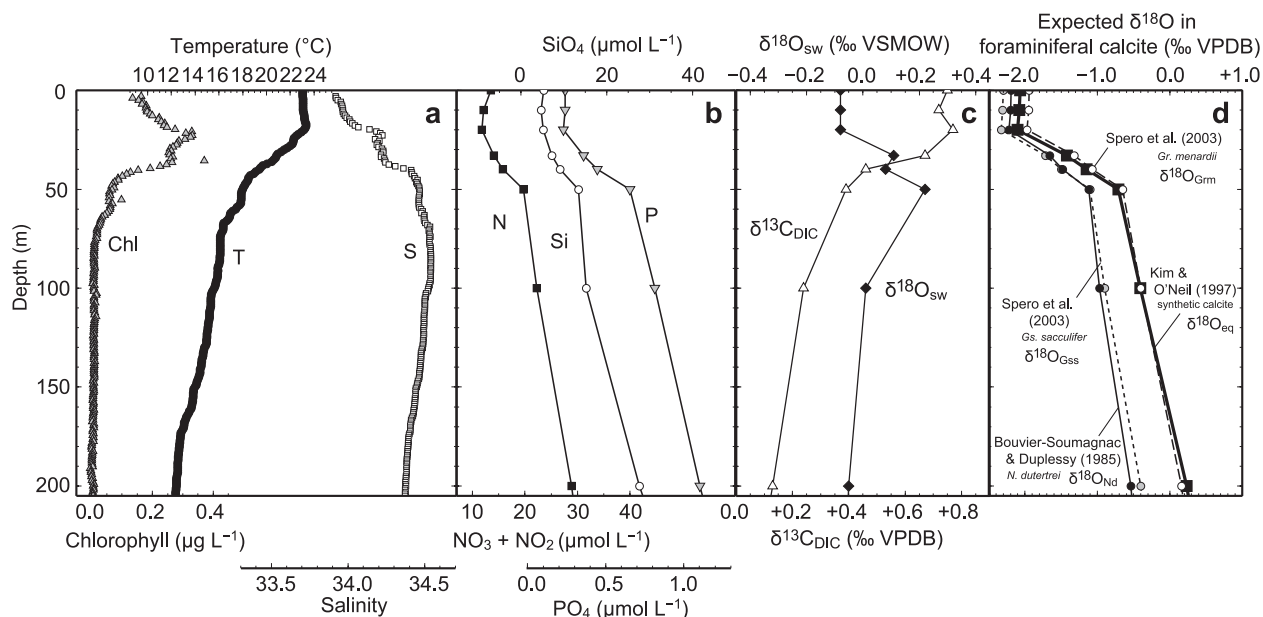


Figure 3. Physical and chemical parameters of the water column at the study site on the sampling day (35°05'N, 139°28'E, 11 October 2011). **a**, Vertical distributions of chlorophyll *a* content (Chl; gray triangles), temperature (T; black circles), and salinity (S; white squares); **b**, vertical distributions of nitrate and nitrite (N; black squares), silicate (Si; white circles), and phosphate (P; gray inverse triangles); **c**, vertical distributions of the oxygen isotope ratio of seawater ($\delta^{18}\text{O}_{\text{sw}}$; white triangles) and the carbon isotope ratio of dissolved inorganic carbon ($\delta^{13}\text{C}_{\text{DIC}}$; black diamonds); **d**, vertical distribution of expected oxygen isotope ratio in foraminiferal calcite. $\delta^{18}\text{O}_{\text{eq}}$, equilibrium calcite (bold line with black squares); $\delta^{18}\text{O}_{\text{Gss}}$, *Gs. sacculifer*-specific fractionation (dashed line with gray circles); $\delta^{18}\text{O}_{\text{Nd}}$, *N. dutertrei*-specific fractionation (broken line with white circles) (see text for detail). *Gs.*, *Globigerinoides*; *N.*, *Neogloboquadrina*; *Gr.*, *Globorotalia*

ues for $\delta^{18}\text{O}_{\text{sw}}$ from the VSMOW scale to the VPDB scale (see Bemis *et al.*, 1998). Equations (4) and (5) were used for *Globigerinoides sacculifer* and *Neogloboquadrina dutertrei*, respectively, because they were calibrated for these specific species. Although eq. (6) was derived from cultured *Globorotalia menardii*, we used it for *Gr. inflata* because it is the only equation established for cultured globorotaliids.

Results

Water column profiles

The water temperature was almost constant (23.0–23.1°C) in the upper 20 m. It decreased sharply with depth to 50 m (to 18.0°C), and decreased gradually below *ca.* 70 m (Figure 3a). Salinity increased rather gradually from the surface to 70 m (to 34.5), showing two sharply increasing intervals at around 18 and 37 m. Salinity decreased gradually below 70 m. The concentration of chlorophyll *a* showed two peaks, the shallower at 18 m (0.33 $\mu\text{g L}^{-1}$) and the deeper at 33 m (0.37 $\mu\text{g L}^{-1}$). These depths nearly corresponded to those of the increases in salinity. The chlorophyll *a* concentration then decreased sharply with depth to 45 m (to 0.06 μg

L^{-1}), and any significant signal was lost below 75 m. The concentrations of nutrients ($\text{NO}_3 + \text{NO}_2$, PO_4 , and SiO_4) were significantly lower in the upper 20 m, increased rapidly to 50 m, and then increased gradually with depth below 50 m (Figure 3b). $\delta^{18}\text{O}_{\text{sw}}$ remained constant in the upper 20 m (–0.1‰), increased to 50 m (+0.2‰), and gradually decreased below 50 m (Figure 3c). $\delta^{13}\text{C}_{\text{DIC}}$ was almost constant in the upper 20 m (*ca.* +0.8‰), then decreased sharply between 20 and 50 m, and decreased gradually with depth below 50 m.

Ontogenetic stable isotope records for foraminifers

Because our foraminifer samples were obtained from a vertically towed natural population, the ontogenetic stages of the individuals may have varied within the same species. Therefore, for the purpose of interindividual comparisons, we used the cumulative test mass as an index of growth (Table 1). The $\delta^{13}\text{C}$ and $\delta^{18}\text{O}$ results for each individual are shown in Figure 4. For each individual, the most ^{18}O -depleted $\delta^{18}\text{O}$ value was always recorded at the smallest chambers (Table 1; Figure 4a). The most ^{18}O -depleted $\delta^{18}\text{O}$ values for each individual ranged from –2.6‰ to –1.9‰ for *Globigerinoides sacculifer* (test mass 2.4–6.1 μg) and from –2.1‰ to

Table 1. Results of the chamber-by-chamber analysis of $\delta^{13}\text{C}$ and $\delta^{18}\text{O}$, and the estimated calcification depth for each chamber. Numbers in parentheses in the “chamber calcification depth” column indicate error intervals for the depth estimation calculated from the $\pm 0.1\%$ analytical error of $\delta^{18}\text{O}$ for each chamber. The presence or absence of a sac-like final chamber is noted in the *Gs. sacculifer* specimens. f, f-1, f-2, ... indicate the chamber positions, counting backward from the final chamber (f). The error of measurement for the test length, calculated from quintuplicate measurements, was $\pm 10\ \mu\text{m}$.

Individuals			Chambers				Equilibrium depth estimation				Species-specific depth estimation				
ID	Sampling depth (m)	Test size (μm)	Chamber position	Chamber mass (μg)	Cumulative test mass (μg)	$\delta^{13}\text{C}$ (‰ VPDB)	$\delta^{18}\text{O}$ (‰ VPDB)	Temperature ($^{\circ}\text{C}$)	Chamber calcification depth (m)	$\delta^{13}\text{C}_{\text{DIC}}$ of corresponding depth (‰ VPDB)	$\Delta\delta^{13}\text{C}_{\text{foram-DIC}}$ (‰ VPDB)	Temperature ($^{\circ}\text{C}$)	Chamber calcification depth (m)	$\delta^{13}\text{C}_{\text{DIC}}$ of corresponding depth (‰ VPDB)	$\Delta\delta^{13}\text{C}_{\text{foram-DIC}}$ (‰ VPDB)
<i>Globigerinoides sacculifer</i>												Spero <i>et al.</i> (2003) <i>Gs. sacculifer</i> equation			
sac1	400–0	500	f	4.7	21.7	+0.9	-1.1	18.9	42 (39–44)	+0.4	+0.5	17.9	55 (48–80)	+0.4	+0.5
(w/ sac)			f-1	9.5	17.0	+0.5	-1.1	19.1	41 (39–44)	+0.5	+0.0	17.9	52 (48–77)	+0.4	+0.1
			f-2	5.0	7.5	+0.3	-1.5	20.9	32 (30–34)	+0.7	-0.4	19.1	41 (38–43)	+0.5	-0.1
			≤ f-3	2.4	2.4	+0.3	-1.9	22.3	24 (22–26)	+0.7	-0.4	21.5	30 (28–32)	+0.7	-0.4
sac2	200–0	750	f	11.2	35.0	+0.9	-1.5	21.2	31 (29–33)	+0.7	+0.2	19.5	39 (36–42)	+0.5	+0.4
(w/o sac)			f-1	10.5	23.8	+0.8	-1.5	20.9	32 (31–35)	+0.7	+0.1	19.1	41 (39–44)	+0.5	+0.3
			f-2	7.2	13.3	+1.0	-1.6	21.7	29 (27–31)	+0.7	+0.3	20.4	36 (33–39)	+0.6	+0.4
			≤ f-3	6.1	6.1	+0.6	-2.0	22.7	22 (21–24)	+0.8	-0.2	22.0	28 (26–30)	+0.7	-0.1
sac3	200–0	610	f	9.0	31.0	+1.4	-1.2	19.5	39 (36–41)	+0.5	+0.9	18.2	48 (45–50)	+0.4	+1.0
(w/o sac)			f-1	12.2	22.0	+1.3	-1.7	22.0	28 (26–30)	+0.7	+0.6	20.7	34 (32–37)	+0.6	+0.6
			f-2	6.3	9.8	+0.9	-2.0	22.7	22 (20–23)	+0.8	+0.2	22.2	27 (24–29)	+0.7	+0.2
			≤ f-3	3.5	3.5	+0.5	-2.1	22.9	21 (19–23)	+0.8	-0.3	22.0	26 (24–28)	+0.7	-0.3
sac4	400–40	640	f	3.1	25.2	+1.4	-1.4	20.7	34 (31–36)	+0.7	+0.8	18.6	43 (40–45)	+0.4	+1.0
(w/o sac)			f-1	7.8	22.1	+0.7	-1.6	21.7	29 (27–31)	+0.7	-0.0	20.4	36 (33–39)	+0.6	+0.1
			f-2	7.8	14.4	+0.7	-1.8	22.2	27 (25–29)	+0.7	-0.1	20.9	32 (30–35)	+0.7	-0.0
			f-3	4.0	6.6	+0.6	-1.8	22.3	25 (23–27)	+0.7	-0.1	21.2	31 (29–33)	+0.7	-0.1
			≤ f-4	2.6	2.6	+0.4	-2.0	22.9	21 (19–23)	+0.8	-0.4	22.0	26 (24–29)	+0.7	-0.3
sac5	200–0	650	f	9.2	28.7	+0.9	-1.1	19.4	40 (38–43)	+0.5	+0.5	18.1	49 (47–65)	+0.4	+0.5
(w/o sac)			f-1	11.3	19.6	+1.0	-1.8	22.2	26 (24–28)	+0.7	+0.3	21.2	31 (29–33)	+0.7	+0.3
			f-2	5.3	8.2	+0.7	-1.7	22.0	28 (26–30)	+0.7	-0.0	20.6	35 (31–38)	+0.6	+0.1
			≤ f-3	2.9	2.9	+0.3	-2.6	—	—	—	—	—	—	—	—
<i>Neogloboquadrina dutertrei</i>												Bouvier-Soumagnac and Duplessy (1985) <i>N. dutertrei</i> equation			
dut1	400–0	430	f	2.7	11.5	+0.7	-1.6	21.5	30 (28–31)	+0.7	+0.0	20.6	35 (32–39)	+0.6	+0.1
			f-1	2.9	8.7	+0.3	-1.2	19.5	39 (36–41)	+0.5	-0.2	18.2	48 (45–57)	+0.4	-0.1
			f-2	1.5	5.8	-0.4	-1.3	20.6	35 (33–38)	+0.6	-1.0	18.5	44 (41–47)	+0.4	-0.8
			f-3	1.8	4.3	-0.2	-1.6	21.5	30 (28–31)	+0.7	-0.9	20.6	35 (31–39)	+0.6	-0.8
			≤ f-4	2.4	2.4	-1.0	-2.1	23.1	20 (18–22)	+0.8	-1.8	22.5	23 (20–25)	+0.7	-1.7
dut2	400–0	450	f	2.7	13.1	+0.4	-1.2	19.5	39 (36–41)	+0.5	-0.1	18.2	48 (45–57)	+0.4	+0.0
			f-1	2.7	10.4	+0.6	-1.4	20.8	33 (31–35)	+0.7	-0.1	19.1	41 (38–44)	+0.5	+0.1
			f-2	2.9	7.6	+0.5	-1.5	21.2	31 (30–33)	+0.7	-0.2	19.5	39 (35–42)	+0.5	+0.0
			f-3	2.4	4.7	-0.1	-2.0	22.7	22 (20–24)	+0.8	-0.8	22.0	26 (23–28)	+0.7	-0.8
			≤ f-4	2.3	2.3	-0.6	-2.0	22.9	21 (19–23)	+0.8	-1.4	22.3	24 (22–27)	+0.7	-1.3
dut3	50–0	520	f	2.1	19.2	+0.1	-1.1	18.9	42 (40–45)	+0.4	-0.3	16.1	73 (49–105)	+0.3	-0.2
			f-1	3.8	17.1	+0.4	-1.1	18.9	42 (39–44)	+0.4	-0.0	16.9	63 (48–97)	+0.4	+0.1
			f-2	6.9	13.3	+0.5	-1.1	18.9	42 (40–44)	+0.4	+0.0	16.4	67 (49–100)	+0.3	+0.1
			f-3	3.1	6.4	+0.2	-1.0	18.6	43 (41–46)	+0.4	-0.3	15.9	90 (57–116)	+0.3	-0.1
			f-4	1.7	3.4	-0.3	-1.7	22.0	28 (26–30)	+0.7	-1.0	20.9	32 (30–35)	+0.7	-0.9
			≤ f-5	1.7	1.7	-1.1	-2.0	22.5	23 (21–25)	+0.7	-1.8	22.0	26 (24–29)	+0.7	-1.8
dut4	33–0	520	f	3.7	15.9	+0.2	-1.2	19.7	38 (36–41)	+0.5	-0.3	18.2	48 (45–50)	+0.4	-0.2
			f-1	4.4	12.2	+0.4	-1.4	20.8	33 (31–35)	+0.7	-0.3	19.1	41 (38–44)	+0.5	-0.0
			f-2	2.9	7.8	+0.1	-1.6	21.5	30 (28–32)	+0.7	-0.6	20.4	36 (33–40)	+0.6	-0.5
			f-3	1.7	4.9	-0.2	-1.7	22.0	28 (26–30)	+0.7	-0.9	20.8	33 (30–36)	+0.7	-0.9
			f-4	1.5	3.2	-0.6	-2.0	22.7	22 (20–24)	+0.8	-1.3	22.3	25 (23–27)	+0.7	-1.3
			≤ f-5	1.7	1.7	-1.0	-2.0	22.5	23 (21–25)	+0.7	-1.8	22.0	26 (24–29)	+0.7	-1.8
<i>Globorotalia inflata</i>												Spero <i>et al.</i> (2003) <i>Gr. menardii</i> equation			
inf1	600–0	510	f	6.6	29.3	-0.2	+0.1	12.6	184 (169–200)	+0.1	-0.3	12.5	195 (177–217)	+0.1	-0.3
			f-1	9.0	22.8	-0.1	-0.2	14.6	136 (120–152)	+0.2	-0.3	14.5	139 (121–157)	+0.2	-0.3
			f-2	7.0	13.7	-0.1	+0.1	12.7	181 (166–197)	+0.2	-0.3	12.5	191 (173–212)	+0.1	-0.3
			f-3	2.4	6.7	-0.5	-0.7	17.9	52 (48–68)	+0.4	-0.9	18.1	49 (46–60)	+0.4	-0.9
			≤ f-4	4.3	4.3	-0.8	-0.7	18.1	50 (48–67)	+0.4	-1.2	18.1	49 (46–58)	+0.4	-1.2
inf2	600–0	440	f	1.5	17.0	—	—	—	—	—	—	—	—	—	—
			f-1	5.2	15.4	+0.1	-0.2	15.0	127 (111–142)	+0.2	-0.1	14.9	129 (111–146)	+0.2	-0.1
			f-2	4.0	10.2	+0.1	-0.2	14.7	134 (119–150)	+0.2	-0.1	14.5	138 (120–155)	+0.2	-0.1
			f-3	2.0	6.3	-0.5	-0.4	15.3	109 (93–125)	+0.2	-0.7	15.3	109 (90–127)	+0.2	-0.8
			≤ f-4	4.3	4.3	-0.5	-0.9	18.5	45 (43–48)	+0.4	-0.9	18.5	44 (41–46)	+0.4	-0.9
inf3	surface	340	f	2.4	5.8	-0.2	-0.6	16.8	65 (50–82)	+0.3	-0.5	17.9	56 (48–76)	+0.4	-0.6
			f-1	1.1	3.4	-0.7	-1.2	19.5	39 (37–42)	+0.5	-1.2	20.0	37 (35–40)	+0.5	-1.2
			f-2	0.8	2.3	-0.7	-1.2	19.5	39 (37–42)	+0.5	-1.2	20.0	37 (35–40)	+0.5	-1.2
			≤ f-3	1.5	1.5	-1.4	-1.4	20.8	33 (31–35)	+0.7	-2.1	21.2	31 (29–33)	+0.7	-2.1

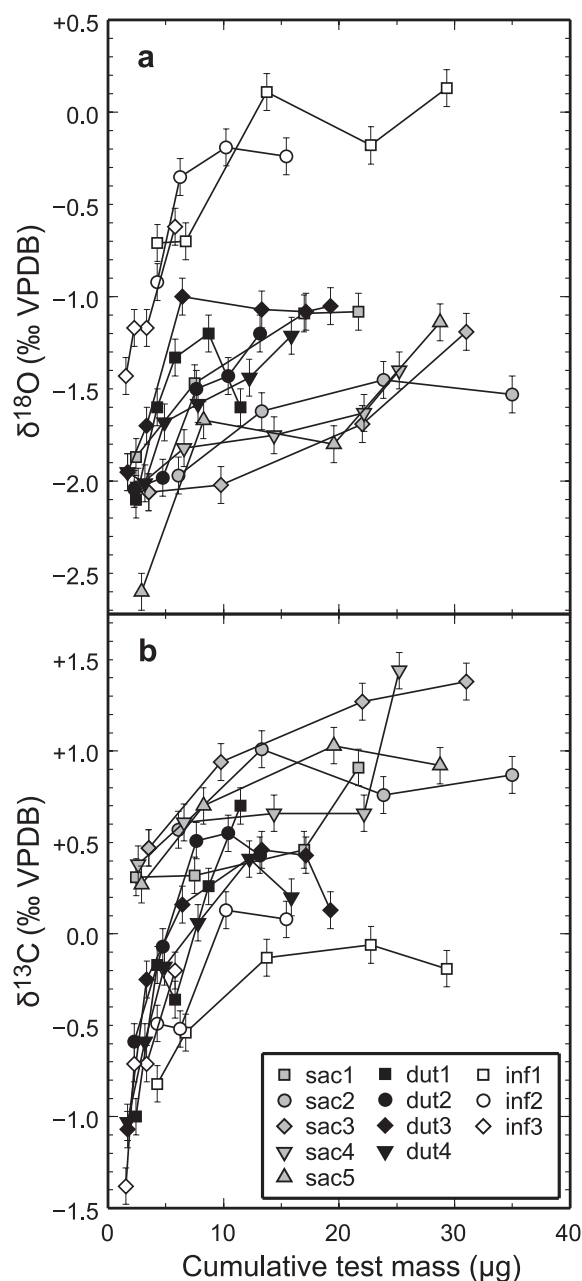


Figure 4. Chamber-by-chamber $\delta^{18}\text{O}$ (a) and $\delta^{13}\text{C}$ (b) versus the cumulative test mass. Data obtained from the same individual are connected in ontogenetic order. The same shade is used for symbols of the same species (gray: *Globigerinoides sacculifer*; black: *Neogloboquadrina dutertrei*; and white: *Globorotalia inflata*). Error bars represent analytical errors ($\pm 0.1\%$).

-2.0% for *Neogloboquadrina dutertrei* (test mass 1.7–2.4 μg). The most ^{18}O -depleted $\delta^{18}\text{O}$ value for *Globorotalia inflata* was higher than those for the other two species, ranging from -1.4% to -0.7% (test mass 1.5–4.3

μg). $\delta^{18}\text{O}$ values tended to become more positive throughout ontogeny in all species (Figure 4a), and this ^{18}O -enrichment was rather rapid in the earlier growth stage (cumulative test mass < ca. 8 μg). The $\delta^{18}\text{O}$ values for *N. dutertrei* and *Gr. inflata* appeared to converge around -1.0% and 0.0% , respectively, at the latest ontogenetic stage observed for each species. For *Gs. sacculifer*, the $\delta^{18}\text{O}$ value for the largest chamber in each individual ranged from -1.5% to -1.1% (test mass 21.7–35.0 μg), representing the most ^{18}O -depleted values among the three species.

The most ^{13}C -depleted values of $\delta^{13}\text{C}$ for each individual corresponded to the smallest chambers, as for ^{18}O -depleted values of $\delta^{18}\text{O}$ (Table 1; Figure 4b). The most ^{13}C -depleted $\delta^{13}\text{C}$ values were $+0.3\%$ to $+0.6\%$ for *Gs. sacculifer* (test mass 2.4–6.1 μg). However, they were much more negative for *N. dutertrei* and *Gr. inflata* relative to that of *Gs. sacculifer* (by at least 0.8%), ranging from -1.1% to -0.6% for *N. dutertrei* (test mass 1.7–2.4 μg) and from -1.4% to -0.5% for *Gr. inflata* (test mass 1.5–4.3 μg). The $\delta^{13}\text{C}$ values of the *Gs. sacculifer* specimens became more positive up to $+0.9\%$ to $+1.4\%$ (test mass 21.7–35.0 μg), although the ontogenetic trajectories varied to some extent among individuals. The $\delta^{13}\text{C}$ values for specimens sac2, sac3, and sac5 tended to become more positive gradually throughout test growth, whereas those for sac1 and sac4 showed large positive shifts in the last chamber (by 0.4% and 0.7% , respectively) (Figure 4b). The $\delta^{13}\text{C}$ values for *N. dutertrei* and *Gr. inflata* became more positive rapidly in the earlier growth stage, up to a cumulative test mass of ca. 12 μg , followed by a slight ^{13}C -depletion. In the largest specimen, infl1 (final test mass 29.3 μg), the $\delta^{13}\text{C}$ value in the final growth stage was -0.2% .

Expected $\delta^{18}\text{O}$ in foraminiferal calcite through the water column

$\delta^{18}\text{O}_{\text{eq}}$, $\delta^{18}\text{O}_{\text{Gss}}$, $\delta^{18}\text{O}_{\text{Nd}}$, and $\delta^{18}\text{O}_{\text{Grm}}$ were calculated from $\delta^{18}\text{O}_{\text{sw}}$ and temperature. Because the variation in $\delta^{18}\text{O}_{\text{sw}}$ in the water column was small ($< 0.3\%$; Figure 3c), the expected $\delta^{18}\text{O}_{\text{eq}}$, $\delta^{18}\text{O}_{\text{Gss}}$, $\delta^{18}\text{O}_{\text{Nd}}$, and $\delta^{18}\text{O}_{\text{Grm}}$ values were controlled mainly by the variation in temperature. They showed almost constant values above 20 m (-2.1%), became more positive rapidly to 50 m, and then gradually below 50 m (Figure 3d).

Discussion

Effect of lamellar structure

Chamber walls of planktic foraminifers usually form a lamellar structure (Reiss, 1958; Bé and Lott, 1964), i.e., a chamber is over-layered by the outer lamella(e) of the subsequently formed chamber(s) (cf. Figure 5). This

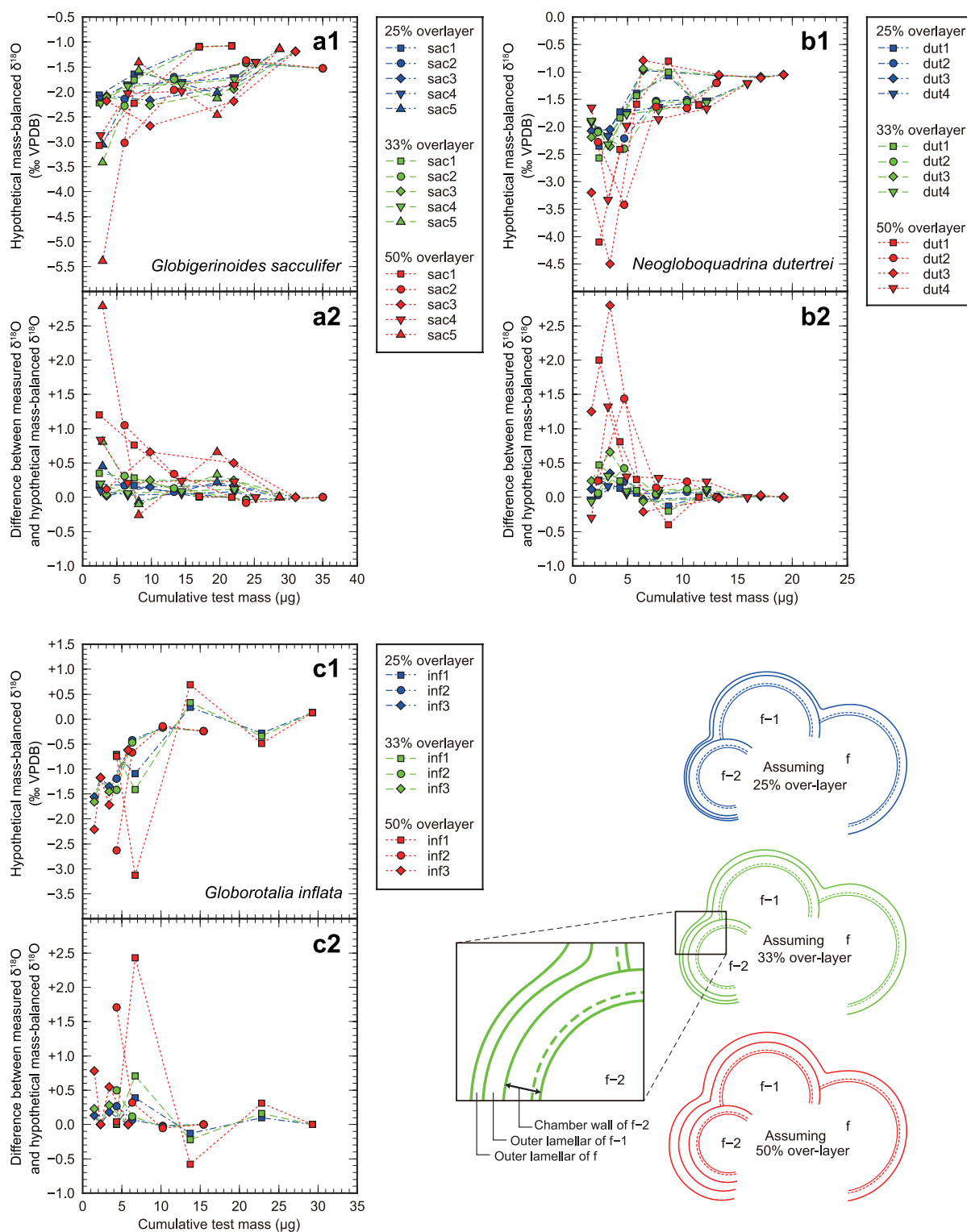


Figure 5. Hypothetical mass-balanced $\delta^{18}\text{O}$ of each chamber at the time the chamber was secreted as the final chamber (a1, b1, c1) and the difference from the $\delta^{18}\text{O}$ actually measured (a2, b2, c2). **a**, *Globigerinoides sacculifer*; **b**, *Neogloboquadrina dutertrei*; **c**, *Globorotalia inflata*. The schematic illustration of the lamellar structure is shown in bottom right. The hypothetical mass-balanced values were calculated at three different scenarios by assuming the ratio of the mass of an existing chamber wall versus that of overlying lamellae of the subsequent chamber for 3:1 (25%), 2:1 (33%), and 1:1 (50%).

means that except for the final chamber, the isotopic signal initially recorded in a calcite wall during the chamber formation is contaminated by those in the later ontogenetic stages. Since the thickness of the over-layering cannot be directly evaluated from the materials utilized in this study, we here modeled three scenarios of relative thickness of the over-layers, which enable us to assess its effect on the bulk-chamber $\delta^{18}\text{O}$ values. For calculating the hypothetical mass-balanced $\delta^{18}\text{O}$ values, we assumed the ratio between the mass of the initially precipitated wall of a given chamber and that of the over-layering lamellae as 3:1 (25% over-layer), 2:1 (33% over-layer), and 1:1 (50% over-layer) (Figure 5).

The variability in each specimen's profile is amplified as the proportion of the over-layer becomes larger (Figure 5a1, b1, c1). With regard to 25%- and 33%-layering models, the $\delta^{18}\text{O}$ differences between the hypothetical mass-balanced values and that of the measured bulk-chambers are small (less than 0.5‰ in most cases). For the 50%-model, however, the modeled $\delta^{18}\text{O}$ values greatly differ from the measured ones especially for earlier chambers (maximum 2.8‰ difference) (Figure 5a2, b2, c2). On the basis of our visual observation, the thickness of the uncovered original wall (septa) of a given chamber is always significantly thicker than 50% of the total thickness of the original wall and the over-layer of the succeeding chamber. Considering the actual wall thickness of the chambers of *Neogloboquadrina dutertrei* we observed under the sample preparation (shown in Figure 2d), it is hard to assume that penultimate chamber has 50% of over-layering. If we assume a given chamber has 50% of over-layering, f-2 and f-3 chambers should have *ca.* 75% and 87.5% of over-layering, which is impractical (Figure 2d). Even in an extreme example of the chamber wall thickness with crust in *N. dutertrei* reported in Steinhardt *et al.* (2015b), the total wall thickness of the f-1 chamber was less than the double to the f chamber. Additionally, since a septum of a chamber is isolated from the surface, over-layering of the succeeding chamber never covers all the area of a given chamber. According to these assumptions, we infer that 50% of over-layering is quite unlikely. Therefore, we hereafter exclude the 50%-model, and at most a 33%-model was considered.

Migration histories through ontogeny

The calcification depth of each chamber was estimated based on the assumption that the foraminiferal calcite analyzed was precipitated under isotopic equilibrium ($\delta^{18}\text{O}_{\text{eq}}$) or by species-specific fractionation ($\delta^{18}\text{O}_{\text{Gss}}$, $\delta^{18}\text{O}_{\text{Nd}}$, and $\delta^{18}\text{O}_{\text{Grm}}$) (Table 1; Figure 5a, b).

For *Globigerinoides sacculifer*, the calcification depth estimated from $\delta^{18}\text{O}_{\text{eq}}$ was slightly shallower than that

estimated from $\delta^{18}\text{O}_{\text{Gss}}$. At the smallest ontogenetic stage analyzed (<5 μg), all the *Gs. sacculifer* specimens calcified their tests within the upper part of the thermocline (shallower than 30 m). With the hypothetical modeled value for 33% over-layer, the calcification depth calculated is equivalent to the mixed layer depth (0–20 m) (Figures 3, 5). Therefore, we estimate that *Gs. sacculifer* analyzed calcified its test within or very close to the mixed layer in their very early stage of ontogeny. *Globigerinoides sacculifer* finally migrated to *ca.* 50 m, which was near the steep decline in chlorophyll *a* content. Among the five specimens analyzed, sac1 had a sac-like chamber in the final chamber position (see Table 1). Because a sac-like shape is an indication of the very-last-formed chamber in this species, the calcification depth of the final chamber of sac1 represents the habitat depth during the terminal stage of its ontogeny. The best estimate of the calcification depth of that sac-like chamber was 42 m (equilibrium estimate) or 55 m (*Gs. sacculifer*-specific estimate). Since the difference between the hypothetical model and bulk $\delta^{18}\text{O}$ is almost negligible in the later ontogenetic stage, deeper migration with ontogeny is a robust finding from our records (Figure 5). Our results for this species are consistent with the deeper migration ecology through ontogeny reconstructed by single chamber Mg/Ca studies using laser ablation techniques (Eggins *et al.*, 2003).

Globigerinoides sacculifer is known to harbor dinoflagellates (*Pelagodinium béii*) in its cytoplasm as obligate symbionts (Hemleben *et al.*, 1989; Shaked and de Vargas, 2006; Siano *et al.*, 2010). Therefore, because its photosynthetic symbionts require light, the vertical distribution of *Gs. sacculifer* is limited by light attenuation. Based on the relationship between light and the chlorophyll *a* concentration in the water column, the bottom depth of the euphotic zone (the depth at which irradiance is 1% of the surface level) can be estimated with the following equation (Morel and Berthon, 1989; Lee *et al.*, 2007):

$$Z_{1\%} = 34.0 \times Chl^{-0.39} \quad (7)$$

where $Z_{1\%}$ is the depth of the euphotic zone and *Chl* is the concentration of chlorophyll *a* ($\mu\text{g L}^{-1}$) at the surface. Using this equation, the depth of the euphotic zone at the study site was calculated to be 69 m. Accepting this estimate, it can be said that *Gs. sacculifer* maintained the photosynthetic capacity of its symbionts throughout its ontogeny, even when it migrated to deeper water in its later ontogeny.

Since the net-collected specimens we analyzed still possessed intact spines (see Figure 2a), they are adult-sized but before reproduction. Once foraminifers reach

reproductive maturation, they should sink within the water column because of loss of buoyancy due to shedding of spines (e.g. Hemleben *et al.*, 1989). Thus it is likely that the terminal descending pathway in each individual is not recorded in our net-collected specimens. Therefore, the deepest habitat depth of matured *Gs. sacculifer* should be much deeper than that estimated from our isotopic records. A previous study using depth-discrete plankton tows (0–200 and 200–600 m) at the Gulf of Aqaba/Eilat, Red Sea, suggested that the release of gametes of *Gs. sacculifer* may occur at 200 m or deeper (Erez *et al.*, 1991). This would also indicate that the very young foraminifers ascend from the deep water to the photic zone. In this respect, this ascending pathway in the beginning of ontogeny after the gametes fusion was not recorded in our results, if very little test carbonate would be precipitated during this ascending pathway. Alternatively, it was masked by the larger mass of the juvenile test precipitated at shallow depth, even if they calcified a small amount of test material. It should be noted that isotopic/geochemical proxies recorded on calcareous tests represent environmental parameters only at the calcification depth. As such, the interpretation of chamber-by-chamber isotopes needs to be done cautiously due to the possibility that the very last and initial phase, i.e., the depth of their reproduction and initial calcification of the new generation, may not be recorded. Since the final calcification, so-called gametogenic calcification (Bé, 1980), may record the depth just before reproduction, analyses of specimens after reproduction obtained by sediment traps and seafloor sediments can possibly provide the habitat depth of their final life stage.

Because of the difference between the equilibrium precipitation equation and the *Neogloboquadrina dutertrei*-specific equation, the estimated calcification depth of *N. dutertrei* showed relatively large variations in colder water. However, the estimated equilibrium calcification depth of *N. dutertrei* was within the thermocline throughout the ontogenetic interval. In contrast, when the *N. dutertrei*-specific equation was used, dut3 was estimated to descend as deep as 90 m and to continue to calcify in the deeper water mass until it formed its final chamber. However, dut3 was collected from the vertical tow of the upper 50 m of water (Table 1). This may indicate that the species-specific equation for *N. dutertrei* produced a too-deep (cold) estimate, at least in our samples, although we cannot exclude the possibility that dut3 ascended within the water column after the calcification of its last chamber. In contrast, the calcification depths of the chambers at a test mass of <3 μg showed well constrained results in the range of 20–26 m, regardless of the equations applied. This depth corresponds to the uppermost part of the thermocline. If we assume 33% over-layer of the sub-

sequent chamber lamellae, the depth in the earlier growth stage (younger than f-3 or f-4) is correlated with the mixed layer. In either case, this species migrated to deeper waters with growth. Compared with the migration profile of *Gs. sacculifer*, the migration toward deeper water is restricted to the earlier stages of its ontogeny. In most cases, if not all, it migrated to the bottom of the level of chlorophyll maximum at a test mass of >10 μg . A number of studies using depth-discrete plankton tows (Fairbanks and Wiebe, 1980; Fairbanks *et al.*, 1982; Kemle-von Mücke and Oberhänsli, 1999) and sediment traps (Erez and Honjo, 1981; Tedesco *et al.*, 2007) have suggested that *N. dutertrei* prefers a water depth near the chlorophyll maximum, where phytoplankton prey is abundant. Our results are consistent with those of previous field studies. These results indicate that the habitat depth of *N. dutertrei* is restricted to within the photic zone throughout its ontogeny, except for the deeper estimate for specimen dut3. In contrast to the obligate symbiosis of *Gs. sacculifer*, which has been studied in detail, the symbiotic nature of *N. dutertrei* is not well known. The ecology of *N. dutertrei* is usually described as “facultative symbiosis” (Hemleben *et al.*, 1989; Spero *et al.*, 2003), which implies that symbionts are not mandatory for this species. Our habitat depth estimate in the euphotic zone does not exclude an obligate photosymbiotic lifestyle for the specimens analyzed. In either case, we conclude that *N. dutertrei* primarily inhabits the thermocline where the chlorophyll *a* concentrations are high.

In the previous reports by Eggins *et al.* (2003), Steinhardt *et al.* (2014, 2015a), an increase of Mg/Ca toward the final chamber was recognized. The profile, in general, implies ontogenetic ascending pathways that contradict the deeper migration suggested from our study and many plankton-tow studies so far conducted (Hemleben *et al.*, 1989). Jonkers *et al.* (2012) also reported an ontogenetic increase in Mg/Ca both in inner layers (ontogenetically precipitated layers) and in the crust of *N. dutertrei*. However, they reported that low Mn/Ca, indicating a deep-water habitat, corresponds to higher Mg/Ca, implying warmer temperature, which is apparently a contradiction. They suggested that the higher Mg/Ca in later ontogenetic stages does not reflect upward migrating pathways. Since the interpretation of Mg/Ca of *N. dutertrei* cannot be straightforward, we refrain from comparison of these studies to our results in terms of its migration history. Future study of single-chamber $\delta^{18}\text{O}$ of cultured specimens under controlled temperature, combined with their Mg/Ca profile is required.

The sizes of the *Globorotalia inflata* specimens analyzed ($n = 3$) differed markedly (Table 1). However, all the specimens descended to deep water. The smallest

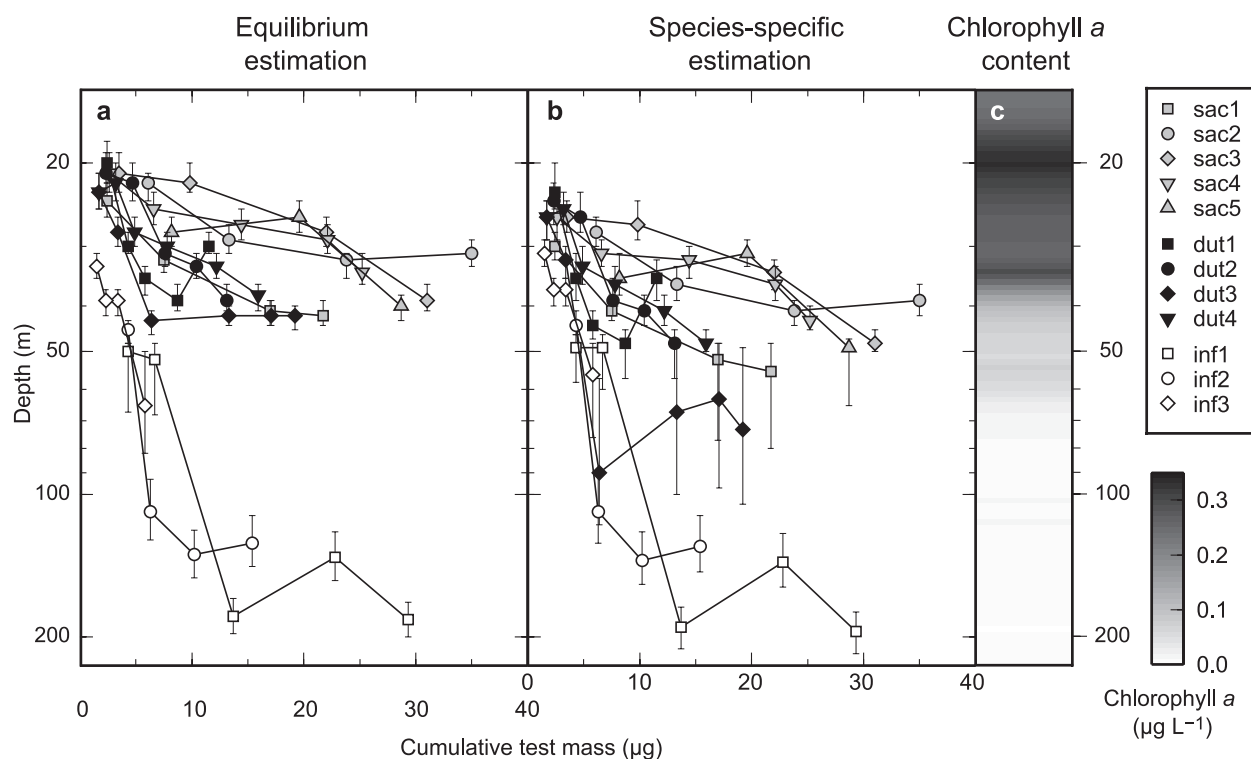


Figure 6. Estimated changes in the calcification depth of foraminifers and comparison with chlorophyll *a* content in the water column. **a**, Calcification depths of foraminiferal chambers estimated with equilibrium precipitation (Kim and O’Neil, 1997). **b**, Calcification depths of foraminiferal chambers estimated with species-specific equations (see text for detail). Data obtained from the same individual are connected in ontogenetic order. The same shade is used for symbols of the same species (gray, *Globigerinoides sacculifer*; black, *Neogloboquadrina dutertrei*; and white, *Globorotalia inflata*). Error bars represent error intervals in the depth estimates calculated from the $\pm 0.1\%$ analytical error of the $\delta^{18}\text{O}$ of each chamber. All estimated depths are listed in Table 1. **c**, Chlorophyll *a* content shown on a monochrome scale. Note that the vertical axis (depth) is on a logarithmic scale to show the upper water column in detail.

specimen, inf3, calcified its smallest chambers in the deeper half of the thermocline, then migrated to just below the thermocline (*ca.* 60 m) at its largest stage (test mass 5.8 μg). The depth trajectory of specimen inf2 also started from the deeper half of the thermocline, and reached its deepest habitat at *ca.* 130 m, with a test mass of >10 μg . The largest specimen, inf1, reached its deepest habitat at *ca.* 200 m, where it calcified its final chamber (at a test mass of 29 μg). The profiles of these three differently sized specimens showed the overall ontogenetic migration profile for this species (Figure 6). Generally, we can say that *Gr. inflata* migrated a great distance from near the bottom of the thermocline to a depth of around 100–200 m, where it remained to calcify several chambers. Thus, the habitat depth of *Gr. inflata* changed from a photic, phytoplankton-rich environment to an aphotic, nutrient-rich environment throughout its life. This type of migration, from shallower to deeper water, in deep-dwelling globorotaliids has also been suggested by depth-discrete plankton tows and the isotopic

characteristics of a series of size-fractionated tests (Lončarić *et al.*, 2006; Wilke *et al.*, 2006; Birch *et al.*, 2013). Moreover, the Mg/Ca study of this species also showed the deepening of the calcification depth (van Raden *et al.*, 2011). Our results reinforced that this profile can be identified even within an individual test.

$\delta^{13}\text{C}$ deviation: relationship to temperature

We calculated the deviations of $\delta^{13}\text{C}$ for the foraminifers from that of DIC (i.e., $\Delta\delta^{13}\text{C}_{\text{foram-DIC}}$) at the estimated calcification depth of each chamber (Table 1). It is noteworthy that the $\Delta\delta^{13}\text{C}_{\text{foram-DIC}}$ values for all the chambers of *Globorotalia inflata* and almost all those of *Neogloboquadrina dutertrei* were negative, ranging between -2.1% and -0.1% and between -1.8% and $+0.1\%$, respectively. In contrast, *Globigerinoides sacculifer* showed much higher values of between -0.4% and $+1.0\%$ (Figure 7). To examine the possible mechanisms underlying these variations in $\Delta\delta^{13}\text{C}$, we considered the $\Delta\delta^{13}\text{C}$ from $\delta^{13}\text{C}$ of the equilibrium inorganic calcite

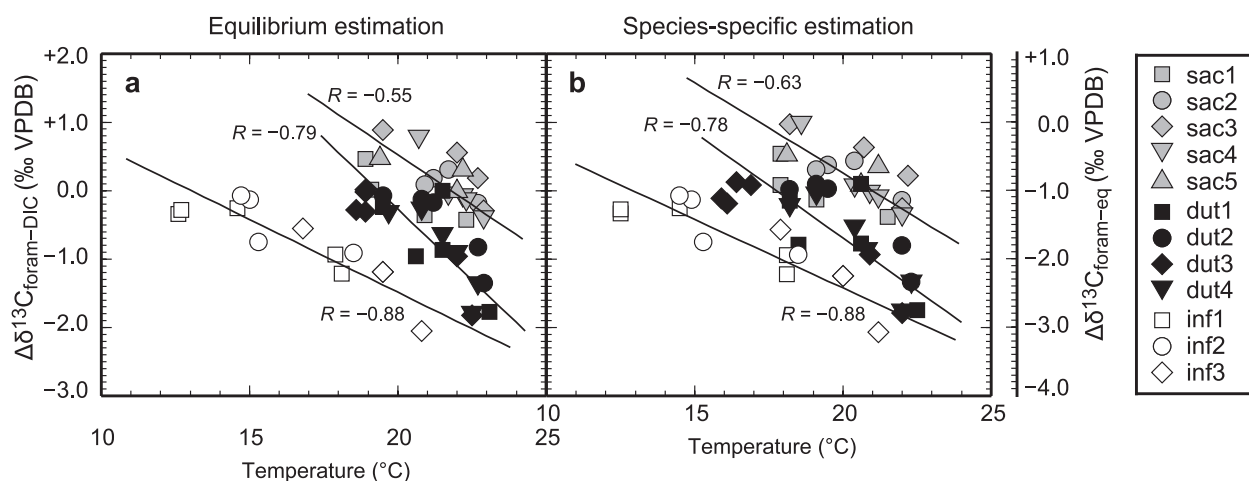


Figure 7. Relationships between the $\delta^{13}\text{C}$ deviation of foraminiferal calcite from $\delta^{13}\text{C}_{\text{DIC}}$ and $\delta^{13}\text{C}_{\text{eq}}$ ($\Delta\delta^{13}\text{C}_{\text{foram-DIC}}/\Delta\delta^{13}\text{C}_{\text{foram-eq}}$) and the estimated calcification temperature. Data are based on the equilibrium estimation of temperature (a), and the species-specific estimation of temperature (b). The same shade is used for symbols of the same species (gray, *Globigerinoides sacculifer*; black, *Neogloboquadrina dutertrei*; and white, *Globorotalia inflata*). $\Delta\delta^{13}\text{C}_{\text{foram-DIC}}$ is scaled on the leftmost axis, and $\Delta\delta^{13}\text{C}_{\text{foram-eq}}$ is scaled on the opposite axis. A significant negative correlation between temperature and $\Delta\delta^{13}\text{C}$ was seen in all species ($p < 0.05$). Lines are reduced major axis regressions. The correlation coefficient (R) is shown next to each line.

rather than from $\delta^{13}\text{C}$ of DIC, because the equilibrium $\delta^{13}\text{C}$ value for inorganically precipitated calcite ($\delta^{13}\text{C}_{\text{eq}}$) is not equal to that of DIC ($\delta^{13}\text{C}_{\text{eq}} = \delta^{13}\text{C}_{\text{DIC}} + 1.0\text{‰}$; Romanek *et al.*, 1992). Figure 7 shows that all the species had negative deviations from the estimated $\delta^{13}\text{C}_{\text{eq}}$ values (see the rightmost scale in Figure 7). Therefore, some process(es) must be generating the negative shift in the $\delta^{13}\text{C}$ of foraminiferal calcite. Three major candidate factors potentially explain these negative deviations from equilibrium: foraminiferal respiration (e.g. Spero and Lea, 1996), kinetic fractionation related to the fast calcification rate (growth rate) (McConnaughey, 1989a, 1989b), and the carbonate chemistry of the calcifying seawater (Spero *et al.*, 1997). The rates of vital activities, such as respiration and growth, are usually a function of temperature. In fact, we found a significant negative correlation between temperature and $\Delta\delta^{13}\text{C}$ in all three species, but the distributions in the plots were species specific (Figure 7). Because the $\delta^{13}\text{C}$ of inorganically precipitated calcite is not dependent on temperature (Romanek *et al.*, 1992), the negative correlation between $\Delta\delta^{13}\text{C}$ and temperature may be attributable to the possible temperature dependence of biological activities; i.e. growth rate and/or respiration rate. It is known that the optimum growth rate shows little temperature dependence over a wide range of temperatures in many foraminiferal species (Caron *et al.*, 1987; Lombard *et al.*, 2009). In contrast, the respiration rates of organisms vary exponentially with temperature, both in theory and prac-

tice (e.g. Brown *et al.*, 2004; López-Urrutia *et al.*, 2006). Such a common mechanism is also expected to occur in planktic foraminifers, and a decrease in $\delta^{13}\text{C}$ in foraminiferal shells has been explained by the greater incorporation of respired $^{12}\text{CO}_2$ at a higher rate of respiration (Berger *et al.*, 1978; Bijma *et al.*, 1990; Spero *et al.*, 1991; Spero and Lea, 1996; Ortiz *et al.*, 1996). Although the mechanism by which the respired CO_2 is finally incorporated into the test is still unclear, the observed negative correlation between temperature and $\Delta\delta^{13}\text{C}$ in our results is consistent with the explanation above. Therefore, we assume that the major contribution to the generation of a temperature-dependent $\Delta\delta^{13}\text{C}$ might be the respiration rate.

$\delta^{13}\text{C}$ deviation: Interspecific differences and ontogenetic trends

As well as the intraspecific changes in $\delta^{13}\text{C}$, interspecific differences were observed (Figure 7). This interspecific segregation cannot be explained by a temperature effect, because the $\delta^{13}\text{C}$ values for each species sharing the same temperature differed significantly. Instead, the species distribution in the plot shown in Figure 7 represents the opposite relationship to temperature; i.e. warmer-water species, such as *Globigerinoides sacculifer*, showed a smaller $\Delta\delta^{13}\text{C}$ deviation than deeper-dwelling *Globorotalia inflata*. This indicates that the difference in $\Delta\delta^{13}\text{C}$ among species largely reflects their species-specific ecology rather than their temperature-dependent

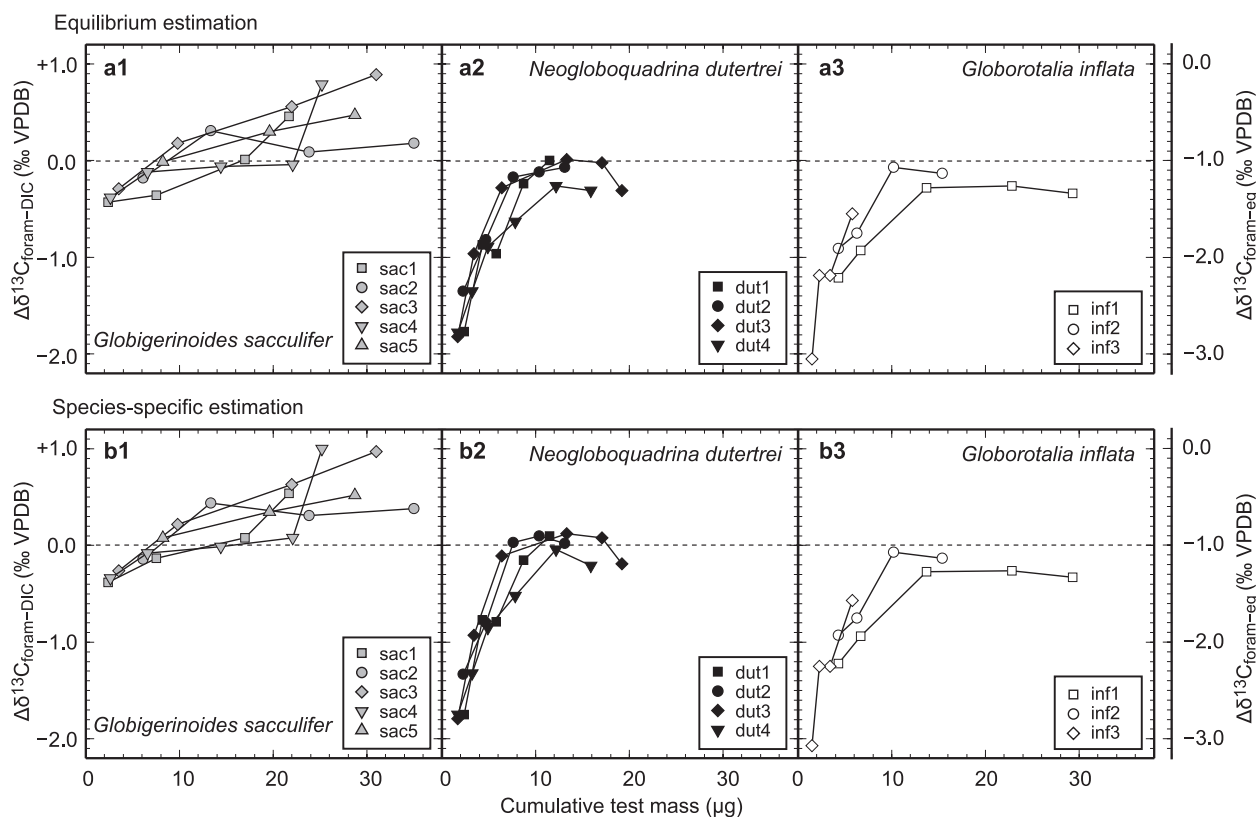


Figure 8. Deviation of the $\delta^{13}\text{C}$ of foraminiferal calcite from $\delta^{13}\text{C}_{\text{DIC}}$ and $\delta^{13}\text{C}_{\text{eq}}$ at the estimated calcification depth ($\Delta\delta^{13}\text{C}_{\text{foram-DIC}}$ / $\Delta\delta^{13}\text{C}_{\text{foram-eq}}$) plotted against the cumulative test mass. $\Delta\delta^{13}\text{C}$ was calculated based on the equilibrium estimation of calcification depth (corresponding to that shown in Figure 7a) (a1–a3), and on the species-specific estimation of calcification depth (corresponding to that shown in Figure 6b) (b1–b3). **a1, b1**, *Globigerinoides sacculifer*; **a2, b2**, *Neogloboquadrina dutertrei*; **a3, b3**, *Globorotalia inflata*. Horizontal broken lines indicate zero deviation from $\delta^{13}\text{C}_{\text{DIC}}$. $\Delta\delta^{13}\text{C}_{\text{foram-DIC}}$ is scaled on the leftmost axis, and $\Delta\delta^{13}\text{C}_{\text{foram-eq}}$ is scaled on the opposite side.

physiological activity. In fact, *Gs. sacculifer* showed higher $\delta^{13}\text{C}$ than *Neogloboquadrina dutertrei*, even though they shared almost the same depth habitat range (temperature range) in the water column (Figures 6, 7).

Of several biological mechanisms that affect $\delta^{13}\text{C}$ of the test, the only effect that makes $\delta^{13}\text{C}$ value more ^{13}C -enriched is symbiont photosynthetic activity (Spero and Lea, 1993; Bijma *et al.*, 1999; Schiebel and Hemleben, 2005), which only affects symbiotic species. Therefore, as expected from their known symbiotic ecology, $\delta^{13}\text{C}$ value was most ^{13}C -enriched in symbiont-bearing *Gs. sacculifer* and most ^{13}C -depleted in asymbiotic *Gr. inflata* (Figure 7). The photosynthetic fixation of carbon by the enzyme ribulose 1,5-biphosphate carboxylase-oxygenase (rubisco) of symbiotic algae preferentially utilizes ^{12}C (O’Leary, 1981). This causes the relative enrichment of ^{13}C in the remaining DIC pool near the foraminiferal test (e.g. Spero *et al.*, 1991; Spero and Lea, 1993; Wolf-Gladrow *et al.*, 1999). This photosynthetic fractionation in the calcifying microenvironments of for-

aminifers explains the differences in $\delta^{13}\text{C}$ observed among species. The $\Delta\delta^{13}\text{C}$ values for *N. dutertrei* were between those for *Gs. sacculifer* and *Gr. inflata*. If the specimens of *N. dutertrei* harbored symbionts, their photosynthetic activity might also have affected the test $\delta^{13}\text{C}$. However, the symbiont effect for *N. dutertrei*, if any, might work in a slightly different way from that proposed for *Gs. sacculifer*. *Globigerinoides sacculifer* radially distributes its symbionts along its densely developed spines, forming a so-called “symbiont halo” (e.g. Hemleben *et al.*, 1989; Bijma *et al.*, 1999; Wolf-Gladrow *et al.*, 1999). The photosynthetic alteration of $\delta^{13}\text{C}_{\text{DIC}}$ within this microenvironment ultimately affects the $\delta^{13}\text{C}$ composition of the test (Spero *et al.*, 1991; Spero and Lea, 1993; Zeebe *et al.*, 1999). In contrast, *N. dutertrei* has no spines to form such a symbiont halo, and its symbionts do not occur outside the test, where the new chamber is formed.

Instead of the above photosynthetic fractionation to enrich the ^{13}C in DIC in the symbiont halo, Bijma *et al.*

(1999) proposed another mechanism to produce the relative enrichment of ^{13}C in DIC by symbiont photosynthesis. Their scenario is, in short, the reduction of the diffusive flux of the respired CO_2 from a foraminifer to the calcifying microenvironment. They proposed that the “scavenging” or utilization of the ^{13}C -depleted respired CO_2 by symbiont photosynthesis can reduce the flux of the respired CO_2 that affects $\delta^{13}\text{C}_{\text{DIC}}$. This is based on the idea that the respired CO_2 commonly affects the foraminiferal calcite to some extent (Berger *et al.*, 1978; Spero *et al.*, 1991; Spero and Lea, 1996). If *N. dutertrei* contains endosymbionts, the higher $\delta^{13}\text{C}$ of *N. dutertrei* relative to that of *Gr. inflata* can be explained by the effective $^{12}\text{CO}_2$ scavenging of its symbionts. Moreover, the much more ^{13}C -enriched $\delta^{13}\text{C}$ values of *Gs. sacculifer* can be explained by the additional effect of the microenvironmental change in $\delta^{13}\text{C}$ attributable to the photosynthetic fractionation within the symbiont halo.

To explain this deviation in accordance with the foraminiferal ontogeny, the $\Delta\delta^{13}\text{C}$ values are shown against the cumulative test masses (Figure 8). All three species showed negative $\Delta\delta^{13}\text{C}_{\text{foram-DIC}}$ values in the earlier ontogenetic stages ($<10\ \mu\text{g}$), and the largest negative $\Delta\delta^{13}\text{C}$ values were observed in the earliest ontogenetic stage in all species. This reflects the higher respiration rate in the relatively warmer habitat the foraminifers experience during early ontogeny. *Neogloboquadrina dutertrei* and *Gr. inflata* showed asymptotic ^{13}C -enrichment in $\delta^{13}\text{C}$ values to near-zero deviation from $\delta^{13}\text{C}_{\text{DIC}}$ during their later ontogeny ($>10\ \mu\text{g}$) (Figure 8). We assume that this saturation in $\Delta\delta^{13}\text{C}$ reflects the decline in metabolic activity as the foraminifers descended to colder waters. Such metabolic deterioration is also a basic principle of organismal ontogeny (Reiss, 1989; West *et al.*, 2001). Thus, these common ontogenetic changes in metabolism also affected the observed asymptotic pattern of $\Delta\delta^{13}\text{C}_{\text{foram-DIC}}$. However, the $\Delta\delta^{13}\text{C}_{\text{foram-DIC}}$ of *Gs. sacculifer* became positive and continued increasing (Figure 8). This profile probably reflects its photosymbiotic activity, which increases as the host grows (Spero and Parker, 1985; Spero *et al.*, 1991; Spero and Lea, 1993; Wolf-Gladrow *et al.*, 1999).

Interestingly, for *N. dutertrei* and *Gr. inflata*, the point of apparent saturation of $\Delta\delta^{13}\text{C}$ can be assigned to a cumulative test mass of around $10\ \mu\text{g}$. At that point, the $\Delta\delta^{13}\text{C}_{\text{foram-DIC}}$ of all three species was around 0‰. Recently, Birch *et al.* (2013) showed that the disequilibrium effect in $\delta^{13}\text{C}$ becomes minimum when foraminiferal specimens of 212–355 μm in test size are used for analyses. Thus, they concluded that this test size window is preferred to reconstruct the past $\delta^{13}\text{C}_{\text{DIC}}$ (Pearson, 2012; Birch *et al.*, 2013). In this study, the cumulative test mass cannot be directly compared to the mesh-size

range proposed in the study above. However, the important fact is that the individual test size, in this case $10\ \mu\text{g}$ in test mass, reflects the $\delta^{13}\text{C}_{\text{DIC}}$ of the water column well, regardless of habitat depths or symbiotic ecology. Thus, our results confirm and reinforce the conclusion of Birch *et al.* (2013) that a certain test size range or mass range can reconstruct past $\delta^{13}\text{C}_{\text{DIC}}$ more accurately over other choices.

Conclusion

We analyzed the chamber-by-chamber $\delta^{13}\text{C}$ and $\delta^{18}\text{O}$ profiles of planktic foraminifers and compared them with the *in situ* environmental parameters of the water column. Based on the assumption of the equilibrium precipitation of chamber $\delta^{18}\text{O}$ or on the species-specific calibrated estimation of $\delta^{18}\text{O}$, we reconstructed the migration histories of individual foraminifers. The very initial stage of ontogeny was not recorded or the record was masked by the larger juvenile chamber subsequently precipitated at shallow depth. The migration records of the all three species started within the thermocline or shallower, where the chlorophyll content is relatively high. They migrated deeper to their final calcification depths, which seemed to be species specific: *Globigerinoides sacculifer* and *Neogloboquadrina dutertrei* migrated to the bottom of the chlorophyll maximum, whereas *Globorotalia inflata* migrated much deeper, to 200 m. Based on the estimated depth of chamber calcification, $\delta^{13}\text{C}$ of *N. dutertrei* and *Gr. inflata* showed considerable negative deviation from the $\delta^{13}\text{C}_{\text{DIC}}$ at the corresponding depth in their earlier ontogenetic stages. However, they showed asymptotic ^{13}C -enrichment in $\delta^{13}\text{C}$ with near-zero deviation from the $\delta^{13}\text{C}_{\text{DIC}}$ in later ontogeny. The narrowing of $\Delta\delta^{13}\text{C}_{\text{foram-DIC}}$ probably reflects a gradual decline in metabolism (reducing the respiration effect) as they migrated to deeper/cooler waters with growth. In *Gs. sacculifer*, $\Delta\delta^{13}\text{C}_{\text{foram-DIC}}$ was also negative during its early ontogeny, although the deviation was smaller than that of *N. dutertrei* or *Gr. inflata*. A subsequent continuous increase in $\Delta\delta^{13}\text{C}$ of *Gs. sacculifer* during its later ontogeny was observed, probably reflecting the photosynthetically induced changes in microenvironmental $\delta^{13}\text{C}$. The $\Delta\delta^{13}\text{C}_{\text{foram-DIC}}$ trajectories of the foraminifers during the course of their ontogeny, in all cases, reached near-zero deviation from $\delta^{13}\text{C}_{\text{DIC}}$ at test masses of around $10\ \mu\text{g}$. The important finding here was that the smallest deviation from $\delta^{13}\text{C}_{\text{DIC}}$ can be assigned to a certain range in test mass regardless of the species ecology, which supports the previous suggestion by Birch *et al.* (2013). Meanwhile, when $\delta^{13}\text{C}$ of foraminiferal calcite is analyzed, larger specimens of symbiotic species with spines hold the

information about symbiont photosynthesis, rather than oceanographic information.

Acknowledgments

We thank the staffs at the Misaki Marine Biological Station (The University of Tokyo) for their support with sampling, and H. Onishi and N. Yoshie (Ehime University) for analyzing the nutrient samples. We appreciate the critical reviews of L. de Nooijer and an anonymous reviewer; the manuscript was greatly improved by their suggestions. We also thank the Editor and the Associate Editor for their kind consideration. This study was supported by JSPS KAKENHI Grant Numbers 24654169 (to K. Moriya), 25701002 (to T. Ishimura), 13J05477 (to H. Takagi), and the Mitsui & Co., Ltd. Environment Fund R08-C019-r (to K. Moriya). The graphs were drawn with Generic Mapping Tools (Wessel and Smith, 1998). All statistical analyses were performed with R (R Core Team, 2014).

References

- Bé, A. W. H., 1977: An ecological, zoogeographic and taxonomic review of Recent planktonic foraminifera. *In*, Ramsay, A. T. S. ed., *Oceanic Micropaleontology*, p. 1–100. Academic Press, London.
- Bé, A. W. H., 1980: Gametogenic calcification in a spinose planktonic foraminifer, *Globigerinoides sacculifer* (Brady). *Marine Micropaleontology*, vol. 5, p. 283–380.
- Bé, A. W. H., Caron, D. A. and Anderson, O. R., 1981: Effects of feeding frequency on life processes of the planktonic foraminifer *Globigerinoides sacculifer* in laboratory culture. *Journal of the Marine Biological Association of the United Kingdom*, vol. 61, p. 257–277.
- Bé, A. W. H. and Lott, L., 1964: Shell growth and structure of planktonic foraminifera. *Science*, vol. 145, p. 823–824.
- Bemis, B. E., Spero, H. J., Bijma, J. and Lea, D. W., 1998: Reevaluation of the oxygen isotopic composition of planktonic foraminifera: experimental results and revised paleotemperature equations. *Paleoceanography*, vol. 13, p. 150–160.
- Berger, W. H., Killingley, J. S. and Vincent, E., 1978: Stable isotopes in deep-sea carbonates: Box Core ERDC-92, west Equatorial Pacific. *Oceanologica Acta*, vol. 1, p. 203–216.
- Bijma, J., Faber, W. W. Jr. and Hemleben, C., 1990: Temperature and salinity limits for growth and survival of some planktonic foraminifera in laboratory cultures. *Journal of Foraminiferal Research*, vol. 20, p. 95–116.
- Bijma, J. and Hemleben, C., 1994: Population dynamics of the planktonic foraminifer *Globigerinoides sacculifer* (Brady) from the central Red Sea. *Deep-Sea Research I*, vol. 41, p. 485–510.
- Bijma, J., Spero, H. J. and Lea, D. W., 1999: Reassessing foraminiferal stable isotope geochemistry: Impact of the oceanic carbonate system (experimental results). *In*, Fischer, G. and Wefer, G. eds., *Use of Proxies in Paleoceanography: Examples from the South Atlantic*, p. 489–512. Springer-Verlag, Berlin.
- Birch, H. B., Coxall, H. K. and Pearson, P. N., 2012: Evolutionary ecology of Early Paleocene planktonic foraminifera: size, depth habitat and symbiosis. *Paleobiology*, vol. 38, p. 374–390.
- Birch, H., Coxall, H. K., Pearson, P. N., Kroon, D. and O'Regan, M., 2013: Planktonic foraminifera stable isotopes and water column structure: Disentangling ecological signals. *Marine Micropaleontology*, vol. 101, p. 127–145.
- Bouvier-Soumagnac, Y. and Duplessy, J. C., 1985: Carbon and oxygen isotopic composition of planktonic foraminifera from laboratory culture, plankton tows and recent sediment: implication for the reconstruction of paleoclimatic conditions and of the global carbon cycle. *Journal of Foraminiferal Research*, vol. 15, p. 302–320.
- Brown, J. H., Gillooly, J. F., Allen, A. P., Savage, V. M. and West, G. B., 2004: Toward a metabolic theory of ecology. *Ecology*, vol. 85, p. 1771–1789.
- Caron, D. A., Bé, A. W. H. and Anderson, O. R., 1981: Effects of variations in light intensity on life processes of the planktonic foraminifer *Globigerinoides sacculifer* in laboratory culture. *Journal of the Marine Biological Association of the United Kingdom*, vol. 62, p. 435–451.
- Caron, D. A., Faber, W. W. Jr. and Bé, A. W. H., 1987: Effect of temperature and salinity on the growth and survival of the planktonic foraminifer *Globigerinoides sacculifer*. *Journal of the Marine Biological Association of the United Kingdom*, vol. 67, p. 323–341.
- Coplen, T. B., Kendall, C. and Hopple, J., 1983: Comparison of stable isotope reference samples. *Nature*, vol. 302, p. 236–238.
- Eggins, S., De Deckker, P. and Marshall, J., 2003: Mg/Ca variation in planktonic foraminifera tests: Implications for reconstructing palaeo-seawater temperature and habitat migration. *Earth and Planetary Science Letters*, vol. 212, p. 291–306.
- Emiliani, C., 1954: Depth habitat of some species of pelagic foraminifera as indicated by oxygen isotope ratio. *American Journal of Science*, vol. 252, p. 149–158.
- Emiliani, C., 1955: Pleistocene temperatures. *Journal of Geology*, vol. 63, p. 538–578.
- Erez, J., Almogi-Labin, A. and Avraham, S., 1991: On the life history of planktonic foraminifera: Lunar reproduction cycle in *Globigerinoides sacculifer* (Brady). *Paleoceanography*, vol. 6, p. 295–306.
- Erez, J. and Honjo, S., 1981: Comparison of isotopic composition of planktonic foraminifera in plankton tows, sediment traps and sediments. *Palaeogeography, Palaeoclimatology, Palaeoecology*, vol. 33, p. 129–156.
- Erez, J. and Luz, B., 1983: Experimental paleotemperature equation for planktonic foraminifera. *Geochimica et Cosmochimica Acta*, vol. 47, p. 1025–1031.
- Fairbanks, R. G., Sverdrlove, M., Free, R., Wiebe, P. H. and Bé, A. W. H., 1982: Vertical distribution and isotopic fractionation of living planktonic foraminifera from the Panama Basin. *Nature*, vol. 298, p. 841–844.
- Fairbanks, R. G. and Wiebe, P. H., 1980: Foraminifera and chlorophyll maximum; vertical distribution, seasonal succession and paleoceanographic significance. *Science*, vol. 209, p. 1524–1526.
- Fairbanks, R. G., Wiebe, P. H. and Bé, A. W. H., 1980: Vertical distribution and isotopic composition of living planktonic foraminifera in the western North Atlantic. *Science*, vol. 207, p. 61–63.
- Friedrich, O., Schiebel, R., Wilson, P. A., Weldeab, S., Beer, C. J., Cooper, M. J. and Fiebig, J., 2012: Influence of test size, water depth, and ecology on Mg/Ca, Sr/Ca, $\delta^{18}\text{O}$ and $\delta^{13}\text{C}$ in nine modern species of planktic foraminifera. *Earth and Planetary Science Letters*, vol. 319–320, p. 133–145.
- Hemleben, C., Spindler, M. and Anderson, O. R., 1989: *Modern Planktonic Foraminifera*, 363 p. Springer-Verlag, New York.
- Ishimura, T., Tsunogai, U. and Gamo, T., 2004: Stable carbon and oxygen isotopic determination of sub-microgram quantities of CaCO_3

- to analyze individual foraminiferal shells. *Rapid Communications in Mass Spectrometry*, vol. 18, p. 2883–2888.
- Ishimura, T., Tsunogai, U. and Nakagawa, F., 2008: Grain-scale heterogeneities in the stable carbon and oxygen isotopic compositions of the international standard calcite materials (NBS 19, NBS 18, IAEA-CO-1, and IAEA-CO-8). *Rapid Communications in Mass Spectrometry*, vol. 22, p. 1925–1932.
- Jonkers, L., de Nooijer, L. J., Reichart, G.-J., Zahn, R. and Brummer, G.-J. A., 2012: Encrustation and trace element composition of *Neogloboquadrina dutertrei* assessed from single chamber analysis—implications for paleotemperature estimates. *Biogeosciences*, vol. 9, p. 4851–4860.
- Kemle-von Mücke, S. and Oberhänsli, H., 1999: The distribution of living planktic foraminifera in relation to southeast Atlantic oceanography. In Fischer, G. and Wefer, G. eds., *Use of Proxies in Paleooceanography: Examples from the South Atlantic*, p. 91–115. Springer-Verlag, Berlin.
- Kim, S. T. and O'Neil, J. R., 1997: Equilibrium and nonequilibrium oxygen isotope effects in synthetic carbonates. *Geochimica et Cosmochimica Acta*, vol. 61, p. 3461–3475.
- Kuroyanagi, A. and Kawahata, H., 2004: Vertical distribution of living planktonic foraminifera in the Japan Sea and northwestern North Pacific Ocean. *Marine Micropaleontology*, vol. 53, p. 173–196.
- Lee, Z., Weidemann, A., Kindle, J., Arnone, R., Carder, K. L. and Davis, C., 2007: Euphotic zone depth: Its derivation and implication to ocean-color remote sensing. *Journal of Geophysical Research*, vol. 112, C03009.
- Lombard, F., Labeyrie, L., Michel, E., Spero, H. J. and Lea, D. W., 2009: Modelling the temperature dependent growth rates of planktic foraminifera. *Marine Micropaleontology*, vol. 70, p. 1–7.
- Lončarić, N., Peeters, F. J. C., Kroon, D. and Brummer, G. J. A., 2006: Oxygen isotope ecology of recent planktic foraminifera at the central Walvis Ridge (SE Atlantic). *Paleoceanography*, vol. 21, PA3009.
- López-Urrutia, A., San Martín, E., Harris, R. P. and Irigoyen, X., 2006: Scaling the metabolic balance of the oceans. *Proceedings of the National Academy of Sciences of the United States of America*, vol. 103, p. 8739–8744.
- McConnaughey, T., 1989a: ^{13}C and ^{18}O isotopic disequilibrium in biological carbonates: I. Patterns. *Geochimica et Cosmochimica Acta*, vol. 53, p. 151–162.
- McConnaughey, T., 1989b: ^{13}C and ^{18}O isotopic disequilibrium in biological carbonates: II. *In vitro* simulation of kinetic isotope effects. *Geochimica et Cosmochimica Acta*, vol. 53, p. 163–171.
- Morel, A. and Berthon, J. F., 1989: Surface pigments, algal biomass profiles, and potential production of the euphotic layer: relationships reinvestigated in review of remote-sensing applications. *Limnology and Oceanography*, vol. 34, p. 1545–1562.
- Mortyn, P. G., Charles, C. D. and Hodell, D. A., 2002: Southern Ocean upper water column structure over the last 140 kyr with emphasis on the glacial terminations. *Global Planetary Change*, vol. 34, p. 241–252.
- Mulitza, S., Boltovskoy, D., Donner, B., Meggers, H., Paul, A. and Wefer, G., 2003: Temperature- $\delta^{18}\text{O}$ relationships of planktonic foraminifera collected from surface waters. *Palaeogeography, Palaeoclimatology, Palaeoecology*, vol. 202, p. 143–152.
- Mulitza, S., Dürkoop, A., Hale, W., Wefer, G. and Niebler, H. S., 1997: Planktonic foraminifera as recorders of past surface-water stratification. *Geology*, vol. 25, p. 335–338.
- Mulitza, S., Rühlemann, C., Bickert, T., Hale, W., Pätzold, J. and Wefer, G., 1998: Late Quaternary $\delta^{13}\text{C}$ gradients and carbonate accumulation in the western equatorial Atlantic. *Earth and Planetary Science Letters*, vol. 155, p. 237–249.
- Norris, R. D., 1996: Symbiosis as an evolutionary innovation in the radiation of Paleocene planktic foraminifera. *Paleobiology*, vol. 22, p. 461–480.
- O'Leary, M. H., 1981: Carbon isotope fractionation in plants. *Phytochemistry*, vol. 4, p. 553–567.
- Ortiz, J. D., Mix, A. C., Rugh, W., Watkins, J. M. and Collier, R. W., 1996: Deep-dwelling planktonic foraminifera of the northeastern Pacific Ocean reveal environmental control of oxygen and carbon isotopic disequilibria. *Geochimica et Cosmochimica Acta*, vol. 60, p. 4509–4523.
- Pearson, P. N., 2012: Oxygen isotopes in foraminifera: overview and historical review. In Ivany, L. and Huber, B. T. eds., *Reconstructing Earth's Deep-Time Climate: The State of the Art in 2012*. Paleontological Society Papers, vol. 18, p. 1–38.
- R Core Team, 2014: R: *A Language and Environment for Statistical Computing*. R Foundation for Statistical Computing, Vienna, Austria, <http://www.R-project.org>.
- Ravelo, A. C. and Fairbanks, R. G., 1992: Oxygen isotopic composition of multiple species of planktonic foraminifera: Recorders of the modern photic zone temperature gradient. *Paleoceanography*, vol. 7, p. 815–831.
- Ravelo, A. C. and Fairbanks, R. G., 1995: Carbon isotopic fractionation in multiple species of planktonic foraminifera from core-tops in the tropical Atlantic. *Journal of Foraminiferal Research*, vol. 25, p. 53–74.
- Reiss, M. J., 1989: *The Allometry of Growth and Reproduction*. 182 p. Cambridge University Press, Cambridge.
- Reiss, Z., 1958: Classification of lamellar foraminifera. *Micropaleontology*, vol. 4, p. 51–70.
- Romanek, C. S., Grossman, E. L. and Morse, J. W., 1992: Carbon isotopic fractionation in synthetic aragonite and calcite: effects of temperature and precipitation rate. *Geochimica et Cosmochimica Acta*, vol. 56, p. 419–430.
- Schiebel, R. and Hemleben, C., 2005: Modern planktic foraminifera. *Paläontologische Zeitschrift*, vol. 79, p. 135–148.
- Shaked, Y. and de Vargas, C., 2006: Pelagic photosymbiosis: rDNA assessment of diversity and evolution of dinoflagellate symbionts and planktonic foraminiferal hosts. *Marine Ecology Progress Series*, vol. 325, p. 59–71.
- Siano, R., Montresor, M., Probert, I., Not, F. and de Vargas, C., 2010: *Pelagodinium* gen. nov. and *P. béii* comb. nov., a dinoflagellate symbiont of planktonic foraminifera. *Protist*, vol. 161, p. 385–399.
- Spero, H. J., Bijma, J., Lea, D. W. and Bemis, B. E., 1997: Effect of seawater carbonate concentration on foraminiferal carbon and oxygen isotopes. *Nature*, vol. 390, p. 497–500.
- Spero, H. J. and Lea, D. W., 1993: Intraspecific stable isotope variability in the planktic foraminifera *Globigerinoides sacculifer*: results from laboratory experiments. *Marine Micropaleontology*, vol. 22, p. 221–234.
- Spero, H. J. and Lea, D. W., 1996: Experimental determination of stable isotope variability in *Globigerina bulloides*: implications for paleoceanographic reconstruction. *Marine Micropaleontology*, vol. 28, p. 231–246.
- Spero, H. J., Lerche, I. and Williams, D. F., 1991: Opening the carbon isotope “vital effect” black box, 2, Quantitative model for interpreting foraminiferal carbon isotope data. *Paleoceanography*, vol. 6, p. 639–655.
- Spero, H. J., Mielke, K. M., Kalve, E. M., Lea, D. W. and Pak, D. K., 2003: Multispecies approach to reconstructing eastern equatorial Pacific thermocline hydrography during the past 360 kyr. *Paleoceanography*, doi: 10.1029/2002PA000814.
- Spero, H. J. and Parker, S. L., 1985: Photosynthesis in the symbiotic

- planktonic foraminifer *Orbulina universa*, and its potential contribution to oceanic primary productivity. *Journal of Foraminiferal Research*, vol. 15, p. 273–281.
- Steinhardt, J., Cléroux, C., de Nooijer, L. J., Brummer, G.-J., Zahn, R., Ganssen, G. and Reichart, G.-J., 2015a: Reconciling single-chamber Mg/Ca with whole-shell $\delta^{18}\text{O}$ in surface to deep-dwelling planktonic foraminifera from the Mozambique Channel. *Biogeosciences*, vol. 12, p. 2411–2429.
- Steinhardt, J., Cléroux, C., Ullgren, J., de Nooijer, L., Durgadoo, J. V., Brummer, G.-J. and Reichart, G.-J., 2014: Anti-cyclonic eddy imprint on calcite geochemistry of several planktonic foraminiferal species in the Mozambique Channel. *Marine Micropaleontology*, vol. 113, p. 20–33.
- Steinhardt, J., de Nooijer, L. L. J., Brummer, G.-J. and Reichart, G.-J., 2015b: Profiling planktonic foraminiferal crust formation. *Geochemistry, Geophysics, Geosystems*, vol. 16, 2409–2430.
- Takagi, H., Moriya, K., Ishimura, T., Suzuki, A., Kawahata, H. and Hirano, H., 2015: Exploring photosymbiotic ecology of planktic foraminifera from chamber-by-chamber isotopic history of individual foraminifera. *Paleobiology*, vol. 41, p. 108–121.
- Tedesco, K., Thunell, R. C., Astor, Y. and Mueller-Karger, F., 2007: The oxygen isotope composition of planktonic foraminifera from the Cariaco Basin, Venezuela: seasonal and interannual variations. *Marine Micropaleontology*, vol. 62, p. 180–193.
- Urey, H. C., 1947: The thermodynamic properties of isotopic substances. *Journal of the Chemical Society*, 1947, p. 562–581.
- van Raden, U. J., Groeneveld, J., Raitzsch, M. and Kucera, M., 2011: Mg/Ca in the planktonic foraminifera *Globorotalia inflata* and *Globigerinoides bulloides* from Western Mediterranean plankton tow and core top samples. *Marine Micropaleontology*, vol. 78, p. 101–112.
- Wessel, P. and Smith, W. H. F., 1998: New, improved version of generic mapping tools released. *Earth & Space Sciences News, Transactions of the American Geophysical Union*, vol. 79, doi: 10.1029/98EO00426.
- West, G. B., Brown, J. H. and Enquist, B. J., 2001: A general model for ontogenetic growth. *Nature*, vol. 413, p. 628–631.
- Wilke, I., Bickert, T. and Peeters, F. J. C., 2006: The influence of seawater carbonate ion concentration $[\text{CO}_3^{2-}]$ on the stable carbon isotope composition of the planktic foraminifera species *Globorotalia inflata*. *Marine Micropaleontology*, vol. 58, p. 243–258.
- Wolf-Gladrow, D. A., Bijma, J. and Zeebe, R. E., 1999: Model simulation of the carbonate chemistry in the microenvironment of symbiont bearing foraminifera. *Marine Chemistry*, vol. 64, p. 181–198.
- Zachos, J., Pagani, M., Sloan, L., Thomas, E. and Billups, K., 2001: Trends, rhythms, and aberrations in global climate 65 Ma to present. *Science*, vol. 292, p. 686–693.
- Zeebe, R. E., Bijma, J. and Wolf-Gladrow, D. A., 1999: A diffusion-reaction model of carbon isotope fractionation in foraminifera. *Marine Chemistry*, vol. 64, p. 199–227.